Theses and Dissertations   1. Thesis and Dissertation Collection, all items

2022-06

UTILIZING EARTH SYSTEMS PREDICTION CAPABILITY (ESPC) TO FORECAST MISTRAL WIND EVENTS

Dahl, Jason C.

Monterey, CA; Naval Postgraduate School

http://hdl.handle.net/10945/70651

NAVAL
POSTGRADUATE
SCHOOL

MONTEREY, CALIFORNIA

THESIS

**UTILIZING EARTH SYSTEMS PREDICTION
CAPABILITY (ESPC) TO FORECAST MISTRAL WIND
EVENTS**

by

Jason C. Dahl

June 2022

Thesis Advisor: Wendell A. Nuss
Co-Advisor: Carolyn Reynolds,
          Naval Research Laboratory-Monterey

Approved for public release. Distribution is unlimited.

THIS PAGE INTENTIONALLY LEFT BLANK

REPORT DOCUMENTATION PAGE			*Form Approved OMB No. 0704-0188*

1. AGENCY USE ONLY *(Leave blank)*	2. REPORT DATE June 2022	3. REPORT TYPE AND DATES COVERED Master's thesis	

4. TITLE AND SUBTITLE UTILIZING EARTH SYSTEMS PREDICTION CAPABILITY (ESPC) TO FORECAST MISTRAL WIND EVENTS		5. FUNDING NUMBERS	
6. AUTHOR(S) Jason C. Dahl			

7. PERFORMING ORGANIZATION NAME(S) AND ADDRESS(ES) Naval Postgraduate School Monterey, CA 93943-5000	8. PERFORMING ORGANIZATION REPORT NUMBER

9. SPONSORING / MONITORING AGENCY NAME(S) AND ADDRESS(ES) N/A	10. SPONSORING / MONITORING AGENCY REPORT NUMBER

12a. DISTRIBUTION / AVAILABILITY STATEMENT Approved for public release. Distribution is unlimited.	12b. DISTRIBUTION CODE A

13. ABSTRACT (maximum 200 words)

Mistral wind events impact the coast of France and build seas in the Gulf of Lion. Strong and persistent wind events impact the routing of naval vessels and the ability to conduct operations in the Mediterranean. Properly identifying the meteorological synoptic picture is key to forecasters seeking to accurately predict Mistral events. Navy Earth Systems Prediction System (ESPC) is a coupled model developed by Naval Research Laboratory to produce atmospheric, oceanographic, and ice sub-seasonal forecasts. Using publicly available deterministic forecasts (from August 2017 through December 2021) and surface pressure and wind analyses, the skill of ESPC and forecast thumb rules in predicting the mistral between 7 and 21 days is evaluated. Deterministic ESPC displays a low amount of skill in directly predicting mistral events two to three weeks ahead. However, using the ESPC prediction of forecaster thumb rules increase the skill in some instances. Analysis of surface pressure and winds over the forecast area for the deterministic forecast was not found to be a reliable method for predicting events beyond the range of typical weather models.

14. SUBJECT TERMS sub-seasonal forecasting, meteorology, synoptic meteorology, Navy Earth Systems Prediction System, ESPC	15. NUMBER OF PAGES 91
	16. PRICE CODE

17. SECURITY CLASSIFICATION OF REPORT Unclassified	18. SECURITY CLASSIFICATION OF THIS PAGE Unclassified	19. SECURITY CLASSIFICATION OF ABSTRACT Unclassified	20. LIMITATION OF ABSTRACT UU

NSN 7540-01-280-5500

Standard Form 298 (Rev. 2-89)
Prescribed by ANSI Std. 239-18

THIS PAGE INTENTIONALLY LEFT BLANK

UTILIZING EARTH SYSTEMS PREDICTION CAPABILITY (ESPC) TO FORECAST MISTRAL WIND EVENTS

Jason C. Dahl
Lieutenant Commander, United States Navy
BS, Old Dominion University, 2013

Submitted in partial fulfillment of the
requirements for the degree of

MASTER OF SCIENCE IN METEOROLOGY AND PHYSICAL OCEANOGRAPHY

from the

**NAVAL POSTGRADUATE SCHOOL
June 2022**

Approved by: Wendell A. Nuss
Advisor

Carolyn Reynolds
Co-Advisor

Wendell A. Nuss
Chair, Department of Meteorology

iii

THIS PAGE INTENTIONALLY LEFT BLANK

ABSTRACT

Mistral wind events impact the coast of France and build seas in the Gulf of Lion. Strong and persistent wind events impact the routing of naval vessels and the ability to conduct operations in the Mediterranean. Properly identifying the meteorological synoptic picture is key to forecasters seeking to accurately predict Mistral events. Navy Earth Systems Prediction System (ESPC) is a coupled model developed by Naval Research Laboratory to produce atmospheric, oceanographic, and ice sub-seasonal forecasts. Using publicly available deterministic forecasts (from August 2017 through December 2021) and surface pressure and wind analyses, the skill of ESPC and forecast thumb rules in predicting the mistral between 7 and 21 days is evaluated. Deterministic ESPC displays a low amount of skill in directly predicting mistral events two to three weeks ahead. However, using the ESPC prediction of forecaster thumb rules increase the skill in some instances. Analysis of surface pressure and winds over the forecast area for the deterministic forecast was not found to be a reliable method for predicting events beyond the range of typical weather models.

THIS PAGE INTENTIONALLY LEFT BLANK

Table of Contents

List of Figures

THIS PAGE INTENTIONALLY LEFT BLANK

List of Tables

THIS PAGE INTENTIONALLY LEFT BLANK

List of Acronyms and Abbreviations

CICE   Community Ice Model

CSI   Critical Success Index

DA   Data Assimilation

ECMWF   European Centre for Medium-Range Weather Forecasts

ENSO   El Niño/Southern Oscillation

ERA5   European Centre for Medium-Range Weather Forecasts (ECMWF) Reanalysis 5th Generation

ESPC   Earth System Prediction Capability

FAR   False Alarm Ratio

GOL   Gulf of Lion

HYCOM   Hybrid Coordinate Ocean Model

IRI   International Research Institute

kts   knots or nautical miles per hour

mb   millibar

METOC   Meteorology and Oceanography

MJO   Madden-Julian Oscillation

NAO   North Atlantic Oscillation

NAVGEM   Navy Global Environmental Model

NDBC   National Data Buoy Center

netCDF   Network Common Data File

NRL	Naval Research Laboratory
NWP	numerical weather prediction
OOD	Officer of the Deck
POD	Probability of Detection
S2S	Sub-seasonal to Seasonal
SR	Success Ratio
SRO	Ship Routing Officer
SubX	The Subseasonal Experiment

Acknowledgments

This thesis is dedicated to the memory of Mr. Patrick Dixon, Senior Meteorologist at Fleet Weather Center-Norfolk and American Patriot, because of whom I am able to present this idea and its use to ship routing and naval operations. For METOC Officers, the caliber of work that we are entrusted with is only dwarfed in comparison with the great people that we are privileged to work alongside. Mr. Dixon embodied what it means to be a professional civil servant and meteorologist. I was fortunate enough to experience what it is like to stand on the shoulders of a giant. I can only hope that this thesis and the remainder of my career honor the life and memory of such a great man.

To my wife and family, thank you for your support and love throughout this process and arduous journey that we call our life together. No one else could be by my side so willingly and without judgement than my wife and family. You all are the reason that the juice is worth the squeeze. I love you all very much.

I also need to thank my advisor, Dr. Wendell Nuss and co-advisor, Dr. Carolyn Reynolds. As a young(er) person, I developed a need to be surrounded by intelligent and capable people which led me to the METOC Community and to the both of you. You have each helped in immense ways during this process and Dr. Nuss, in particular, has displayed the requisite patience needed for sainthood.

THIS PAGE INTENTIONALLY LEFT BLANK

CHAPTER 1:
Introduction

1.1 Motivation

While standing watch as a Ship Routing Officer (SRO), I was contacted by the captain of a ship that had low operational limits for wind intensity in sea heights. This is a common occurrence given the constraints of his vessel. He inquired as to whether or not their intention to operate within the Gulf of Lion (GOL) would be impacted by any arduous weather conditions that could cause sea heights and wind intensity to be over the prescribed intensity for his vessel. Normally, that inquiry would be met with resistance due to a well-advertised five to ten day limitation with modern numerical modeling. All of the ships that we supported are restricted to forecasts of five to ten days due to the limitations of numerical weather prediction (NWP). Large amounts of time, money, and resources are impacted by the certainty of ship routing therefor high levels of certainty are paramount.

A skilled forecaster with NWP models can reasonably forecast the synoptic scale pattern out to 5 or 6 days with decreasing skill as the lead time increases. How fast the forecast degrades is a function of the skill of the forecaster, NWP model(s), and forecast method that is being employed. But the specificity of this question intrigued me because the only feature that I could see impacting the GOL was a Mistral Wind Event. Mistrals are a strong northwesterly wind event brought on by synoptic conditions over the European continent and Mediterranean.

Earlier in the week, I had participated in a visit from Naval Research Laboratory-Monterey and was introduced to the Navy Earth System Prediction Capability (ESPC) and its ability to provide a link between climatology and weather. The concept was that by coupling our global ocean and sea ice forecast models together with our global atmospheric forecast model, we could get skillful daily averages of environmental conditions at longer forecast times than we could get from the atmospheric model alone. This is because the ocean and sea ice evolve more slowly than the atmosphere, and impart some forecast skill to the atmosphere at longer forecast lead times. This would enable us to get a rough estimate of

the environment at ranges beyond current weather forecast timescales.

With that in mind, I decided to look at the model output and see if it could answer the captain's inquiry by re-framing it into one simple question: "Is a Mistral wind event likely to occur in 10-14 days or will the synoptic setup not produce such an event?" By simplifying the inquiry to one specific area and well-known weather event, would I be able to increase the time frame in which to take action and alter the ship's route thereby saving time and resources?

I was able to access the model output online via The Subseasonal Experiment (SubX) website and see an increase in northwesterly winds in the vicinity of the GOL during the days of the captain's planned exercise. The model was a mosaic of data that I was not accustomed to viewing but I could see a granular version of what the ensemble of NWP models had produced with a clear forecast of the synoptic picture. I quickly used what I had learned in the visit and the personal experience that I had as an Officer of the Deck (OOD) on my first commissioned sea tour a few years prior to inform the captain of the possibility of a Mistral and likely impacts to his vessel. The model indicated that an increase in wind speed caused by a ridge of high pressure from the west-northwest would interact with a developing low pressure system around two weeks from that time. The event did in fact occur and the ship eventually had to make port to avoid the high wind and seas instead of participate in their exercise. It was then that I began to think about the likelihood that I could replicate this situation and increase the time frame in which these events could be forecast and allow for increased planning and knowledge for others who may face a similar situation.

Weather forecasting can be described as the act of predicting the state of the atmosphere at a particular time and location using science and technology (Iseh and Woma, 2013). In this description, the task of predicting the future environmental conditions is relative to the tools at the forecaster's disposal. The appropriateness of the data given to the forecaster for their particular time and place is a balance of the time and detail needed to produce the product. As computing technology improves, the detail and scale in which the forecast models are able to resolve phenomena will follow suit.

This research is motivated by the experience of having to answer the question posed to me

by the ship captain. The hope is to highlight the utility and/or difficulty in using ESPC to forecast synoptic level events such as the Mistral. The basis of the study is to take existing forecast techniques and apply these methods using ESPC's forecast data in the sub-seasonal range. In doing so, we can hopefully highlight the ability of ESPC to detect synoptic level atmospheric patterns and provide SROs and forecasters with an example of proper utilization of this model in support of naval operations.

1.2 Hypothesis

I believe that by applying synoptic scale forecast criteria, based on the positions of high and low pressure systems relative to the GOL, to ESPC ensemble predictions we will be able to produce a relatively accurate outlook for the likelihood of a Mistral event to occur in a 7-21 day forecast window. I also believe that by using specific criteria, from forecaster thumb rules, we will be able to improve the skill of Mistral wind event predictions over raw model wind predictions. In doing so, we will provide an example in which the Meteorology and Oceanography (METOC) community can enhance planning efforts by providing guidance of environmental impacts to operations when the meteorological mechanisms are at a suitable scale for ESPC to resolve.

1.3 Assumptions and Constraints

Based on the limitations of the daily averaged forecast model output, and the chaotic nature of the atmosphere limiting the forecast skill for brief or weak mistral events, we apply a constraint on the events we consider here and make assumptions about their impact. First, we are targeting our study with respect to Mistral events that have at least a one day duration. The nature of our ESPC forecast model is that it produces daily averages and an event of a few hours that isn't intense may be hard to detect in averaged daily forecast values. Secondly, we are assuming that the event perfectly coincides with a ship's intended path. This is more of a Naval operational assumption but either way must be congruent with an event that we detect or study. Finally, in the interest of applicability to all Naval vessels and not just the lower operating limit ships, we need to find intense or long lasting wind events with a premium placed on those that meet both. Such events can be anomalies when compared to climatology and getting the significance and duration of these events correctly

3

when predicting their occurrence must be regarded as a successful demonstration of ESPC's ability beyond climatology and at a longer interval than NWP.

CHAPTER 2:
Background

2.1 Mediterranean Winds

The Mediterranean Sea is an area of natural cyclogenesis that is characterized by synoptic scale activity and impacted by orographic features such as mountain ranges and unique sea-air interactions. These features coupled with synoptic variability make forecasting wind and seas difficult (Reiter, 1975). At the time of this cited forecasting guide, the author noted the challenges of the synoptic variability based on seasonal oscillations as one of the main causes in difficulty for forecasters. Modern NWP models have resolved much of the short term uncertainty with high resolution grid spacing and advanced physics packages but only once the synoptic conditions are known in the 1-5 day timeline. For these dynamic wind events with detailed topography requiring complex parameterization, sub-grid scale processes, and high-resolution data assimilation, the time scales and spatial resolution are down to the hour/minute and few kilometer grid resolution. The true challenge for maritime forecasters lies in being able to accurately predict the synoptic pattern and accurately interpret the intensity of each wind regime with enough time to reposition assets transiting through the area.

Figure 2.1. Reiter (1975) identified the various wind regimes in the
Mediterranean Sea with their direction. All of these regimes are based
on a relationship between synoptic scale forces and orographic features
between the land mass and coastline maritime environment. Adapted from
Reiter (1975)

For Naval fleets and commercial shipping, the Mediterranean presents a unique environment
in which to operate and one that is worthy of study. The area must be transited before
reaching the Suez Canal and entering the Red Sea for east bound transiting units as well
as west bound groups returning to homeport. Due to the relatively smaller operating area
that the Mediterranean possesses when compared to the Pacific and Atlantic theatres, the
solution when facing a dynamic wind event is to place ships in port or alter the speed at
which they transit the area. Both solutions require early warning to provide the commander
with the decision time needed to adjust his/her intentions and follow-on impacts of that
decision. If the METOC community can provide earlier guidance to the commander that
would enable an exercise, port visit, or restrictive meteorological conditions to be provided
on a scale of a few weeks rather than 5 days, it is worth exploring what that would take and
with what accuracy it can be done.

2.2   Forecaster Thumb Rules

"Necessity is the mother of invention" is a phrase that has been adopted from a writing by Plato into the English lexicon. The simple yet elegant adage can be applied to why so called "thumb rules" have been developed by forecasters over time and careful study. Brody and Nestor (1980), in their study, sought to create thumb rules for every wind regime in the Mediterranean based on observed trends from satellite and observation data and thereby give forecasters an indication of whether the synoptic conditions existed for the onset of wind regimes.

Thumb rules themselves are not necessarily rooted in scientific theory but often the rules can be indicators of proven physical relationships between observed parameters in the environment. For the Brody and Nestor (1980) Mistral thumb rules, they developed onset, intensity, and cessation thumb rules. Onset rules were designed to be predictive of an event whether it was a few days or hours and the intensity rules were indications of the strength of the Mistral winds that were taking place. Cessation rules were indications that the event was likely to end. Forecasters, through necessity, have developed these thumb rules based on careful study of the observed relationships between different observation stations and a simple application of physics, such as conservation of mass, in an effort to make predictions based on sound meteorological and scientific reasoning.

While thumb rules have effectively been supplanted by NWP, their application to numerical model output provides a check on the accuracy of the forecast. The Brody and Nestor (1980) thumb rules assess various forecast parameters at the locations shown in Fig. 2.2 and consist of the following.

1. 500 mb winds at Brest or Bordeaux are northwesterly at 65 knots or nautical miles per hour (kts) or greater.
2. 850 mb winds at Nîmes are northerly at 50 kts.
3. Sea level pressure differences between Perpignan, Marseille and Nice are greater than 3 millibar (mb) or 6 mb between Perpignan and Nice.

When these rules meet specific criteria, a forecast of Mistral winds is indicated. If the thumb rules are accurate, then the application of these thumb rules to numerical model predictions should highlight when model predicted winds in the GOL are associated with a Mistral

event. The application of these thumb rules may overcome some model forecast errors by identifying a Mistral regime based on larger scale features even when the model fails to predict the correct Mistral surface winds directly.

2.3 Mistral Wind Events

The Mistral wind event is described as a strong northwesterly to northerly katabatic wind event that impacts the entire coast of the GOL. This wind brings cold and dry air from the Bay of Biscay through the Rhône Valley, Carcassone Gap, and Durance Valley (Brody and Nestor, 1980). These events can bring storm and gale force winds accompanied by rough seas to the maritime region of Southern France and extend into the Tyrrhenian and Ionian Seas. Some studies have sought to distinguish these events into two categories of Mistral and Tramontane based on the orographic path taken by the winds to reach the Gulf of Lion. For our purposes, we will refer to them as simply one Mistral wind event as it is displayed in Fig. 2.1. Brody and Nestor (1980) also identified the three synoptic setups to describe the mid-level synoptic wind pattern required to produce northwesterly winds in the GOL. A key aspect of these synoptic regimes is that they all support an along-coast surface pressure gradient from Italy to Spain, which supports northwesterly surface winds.

Figure 2.2. Locations of Brest, Bordeaux, Nîmes, Perpignan, Marseille, and Nice (Google, 2022).

Type A: Blocking Ridge
and short wave trough
over Eastern Europe
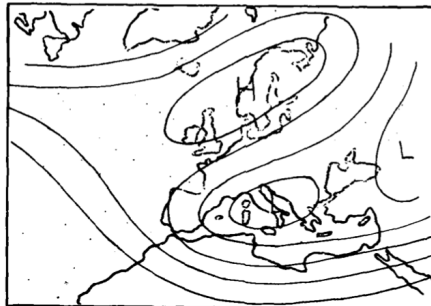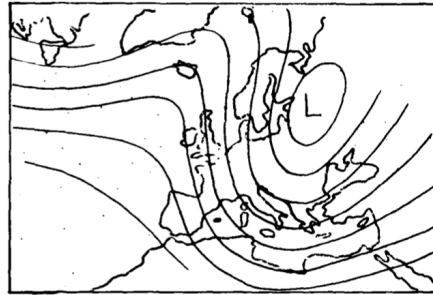
Type B: Blocking Ridge
enhanced by low pressure
system over Italian Peninsula
(Genoa Low)

Type C: Series of lower
level troughs over continent
and mid-level zonal flow
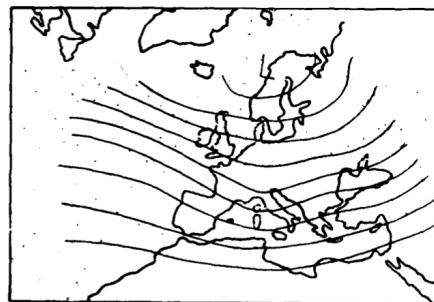
Figure 2.3. Brody and Nestor (1980) identified three different synoptic patterns in which Mistral Wind events are most likely to occur. Adapted from: Brody and Nestor (1980)

According to climatology, Mistral winds can last anywhere from a few days to almost two weeks and occur as many as 15 times a month (Givon et al., 2021) as shown in Fig. 2.4. The frequency of these events has been studied in order to show wind power generation and grid resiliency as well as the implications from climate change (Dedecca et al., 2016) .

10
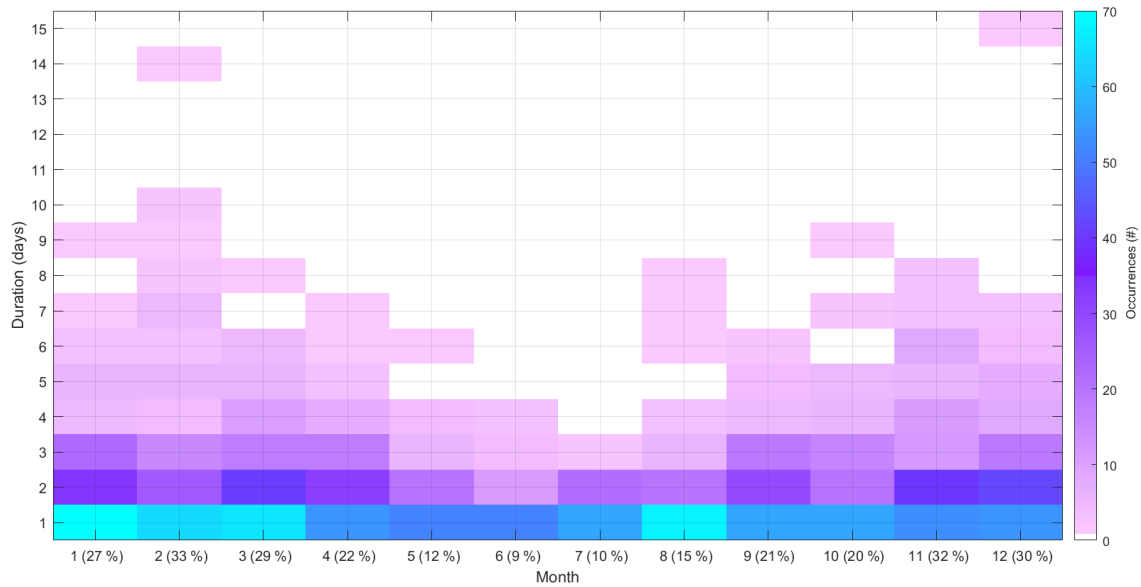
Figure 2.4. This plot shows the frequency and duration of Mistral events over all 12 months from 1981-2016 (Givon et al., 2021).

To set a minimum wind speed criteria to define an operationally significant Mistral, the impact on ocean waves was considered. Considering the approximate 300 nautical mile fetch area and wind speed duration of at least 24 hours shown in 2.5, we used a wave nomogram to define a minimum daily wind speed of a Mistral of 18 knot wind speed to produce 7-8 feet significant wave height seas (Bretschneider, 1970). For our purposes, we defined a Mistral event as being one with winds from 310°-340° at a minimum of 18 kts. This method allows for a minimum daily wind speed threshold that could conceivably impact an operation over one or several days.
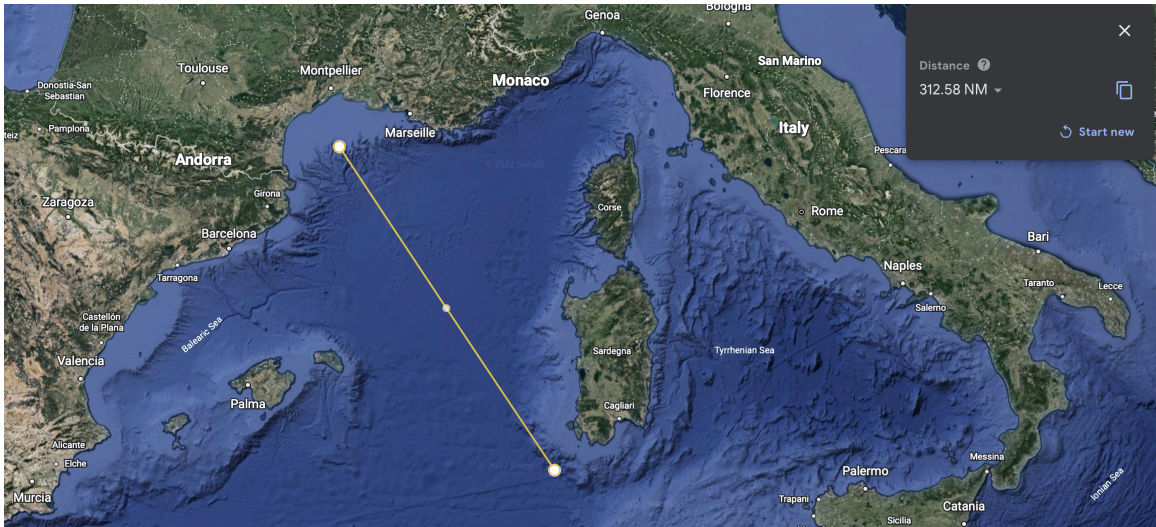
Figure 2.5. Google Earth Image of Gulf of Lion area showing the approximately 300 nautical mile fetch area for a Mistral available to propagate seas and path into Tyrrhenian and Ionian Seas (Google, 2022).
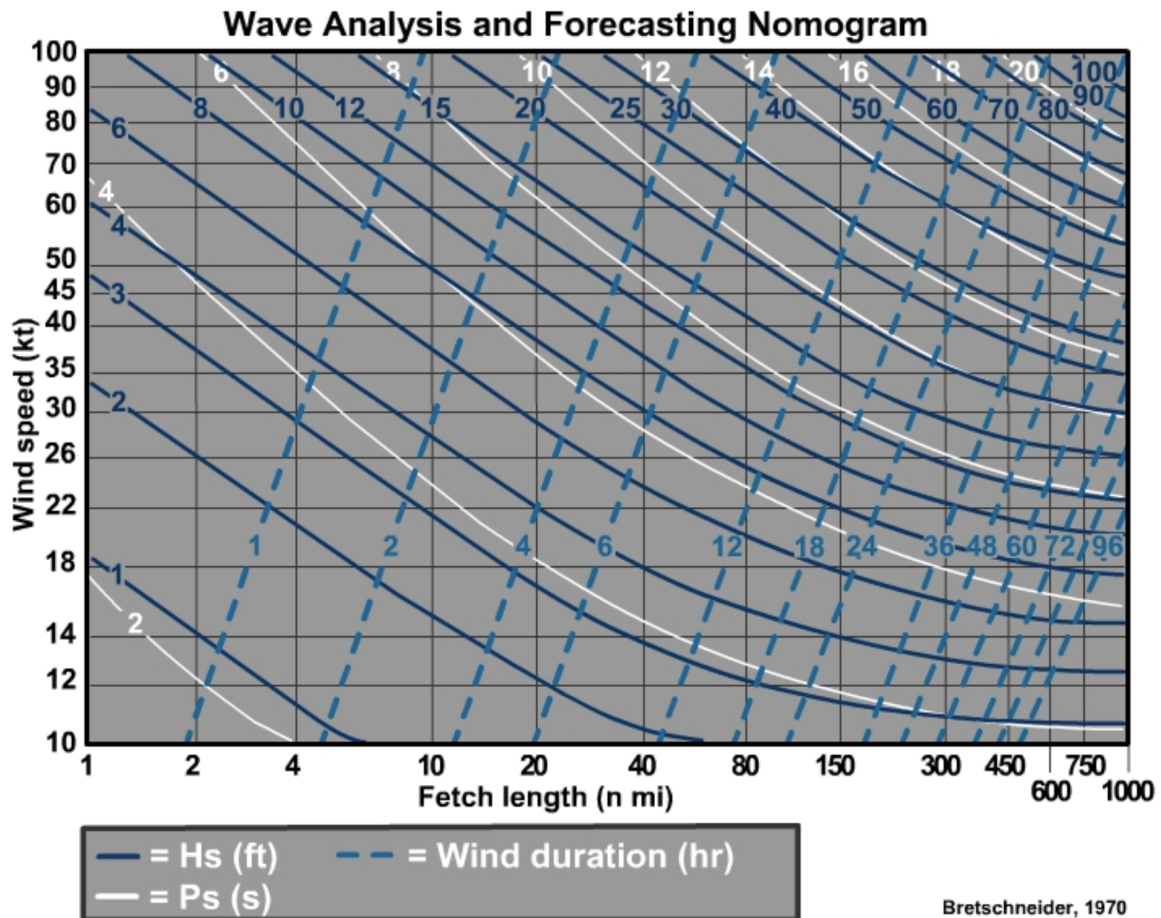
Figure 2.6. Wave nomogram showing relationship between fetch area, wind speed, and duration of winds to yield significant wave height Adapted from: Bretschneider (1970).

Using temporally-smoothed data (daily averaged) will mean we cannot distinguish between short intense events and longer less intense events. However, since the net effect is the same, the production of rough seas and high winds, using daily-averaged data will allow us to identify significant events. Mistral events that occur for days at a time are more relevant to ship routing and naval operations as well. By using daily averaged winds, we are able to identify key events relevant to the synoptic picture.

2.4 North Atlantic Oscillation and Mistral Wind Events

The North Atlantic Oscillation (NAO) refers to the large scale alternation of atmospheric mass between the North Atlantic and semi-permanent high pressure system normally located over the Azores (Lamb and Peppler, 1987). This seasonal oscillation can cause an unusually tighter meridional gradients between the Azores high pressure system and low pressure systems passing to the north at the 500 mb pressure level. This anomalous relationship is west-northwest of the GOL depending on the season and has a major impact on the synoptic pattern. Like most oscillations, the NAO is described by the phase of the oscillation. A positive phase represents anomalous higher pressure and lower pressure of both systems, indicating a tighter gradient and in turn forcing the polar front jet to a more meridional pattern. A negative phase represents the opposite, which weakens the high and low pressure systems creating a weak gradient and promoting a zonal pattern to the jet. Both phases of the NAO impact the synoptic weather pattern in the North Atlantic and thereby impact the pattern needed to produce a Mistral.

For our three synoptic setups, Types A and B are dependent upon the ridge of high pressure to force anticyclonic winds into the mountain gaps and create the northwesterly winds needed for a Mistral. A positive phase NAO creates this enhancement and builds a stronger high pressure system. Figure 2.3 shows that the relative position of the high and the presence of the Genoa Low are the main differences between the two synoptic setups. However, both types are enhanced by a positive phase NAO. Alternatively, for a Type C Mistral, a weakened Azores high and thus more zonal jet pattern with westerly flow would be enhanced during a negative phase NAO cycle. Nevertheless, the phase of the oscillation impacts the relative strength of the Azores high and thus determines which synoptic pattern is more likely to occur and, based upon that, which type of Mistral is most likely to occur. Fig. 2.7 shows that the NAO undergoes amplitude changes on weekly cycles with some resulting in rapid phase changes. Although beyond the scope of the present study, these NAO amplitude and phase changes likely impact Mistral events and need to be captured by model forecasts.
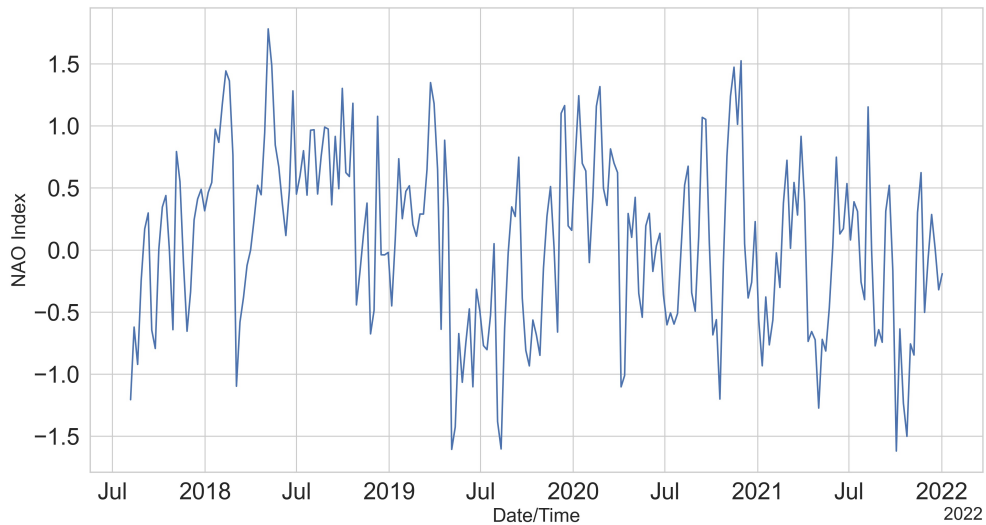
Figure 2.7. This plot shows the weekly average NAO Index from August 5th, 2017 to December 31st, 2021 (Data Source: Climate Prediction Center).

2.5 Sub-seasonal to Seasonal Forecasting

Sub-seasonal to Seasonal (S2S) forecasting is a growing area of research and is being used operationally to address various meteorologic and oceanographic events such as tropical cyclones (Janiga et al., 2018), Asian Summer Monsoon (Liang and Lin, 2018), and Arctic sea ice thickness (Allard et al., 2020). Limitations of weather and climate modeling efforts are partly due to our limited understanding of the interactions between different earth system components and our ability to properly represent these interactions numerically within the models themselves (Hurrell et al., 2009). In order to increase atmospheric prediction windows beyond current timescales, coupling the atmosphere to the more slowly evolving components of the ocean and sea ice dynamics while allowing the components to interact in these time scales is needed. This approach allows us to extend useful forecasts to weekly timescales for slowly evolving coupled oscillations such as the Madden-Julian Oscillation (MJO). Several authors have made the case for the development of "seamless"

earth system prediction capabilities to overcome artificial differences between weather and climate models, and allow for skillful forecasts on S2S timescales (e.g., Brunet et al. (2010); Shapiro et al. (2010); Ruti et al. (2020)). Realizing the potential of S2S forecasting is the result of years of model development, advances in computing power, and climate research being leveraged into an ensemble of model data and coalesced into a useful forecast tool. Numerical weather models have gained complexity and accuracy with the advent of super-computing and advances in Data Assimilation (DA) and coupling of the shorter time scale earth system components. Decades of climate research resulted in the discovery of other seasonal oscillations in addition to the NAO to include the MJO (Madden and Julian, 1972) and, most importantly, El Niño/Southern Oscillation (ENSO) (Walker and Bliss, 1933). The marrying of the efforts of NWP in atmospheric and oceanographic modeling capabilities to the known seasonal oscillations at longer time scales has driven S2S capabilities and modeling efforts.

2.6   Navy Earth System Prediction Capability

ESPC is the Navy's S2S forecast model and has been developed by Naval Research Laboratory (NRL) since 2010 (Eleuterio and Sandgathe, 2012). The model employs a coupled framework developed by Theurich et al. (2016) in order to allow interaction with the global atmospheric, ocean, and ice models (Barton et al., 2019). The atmospheric component of ESPC is Navy Global Environmental Model (NAVGEM), the oceanographic component is Hybrid Coordinate Ocean Model (HYCOM) (Chassignet et al., 2007), and the ice model is the Community Ice Model (CICE) (Hunke et al., 2008). These components are coupled by input and output and permitted to interact as shown in Figure 2.8. Additionally, ESPC employs a loosely coupled DA approach as shown in Figure 2.8. This method enables the data to be assimilated into the model at a staggered approach and keeps the DA process in the ocean/ice and atmospheric models separate. Also, the model uses a perturbed observation approach to the forecast-assimilation cycle where each ensemble member maintains its own ability to add perturbations to the observations separately. This allows for a normal distribution of error across the members of the ensemble while applying a statistical approach to error over the several interactions between the ensemble members (Barton et al., 2019). This approach to ensemble modeling at the S2S time-scale is necessary given the inherently complex interactions taking place on the ocean/ice systems and atmospheric processes over

such a long time frame while accounting for seasonal oscillations. The S2S approach and ESPC specifically is used in this study to extend the potential Mistral forecasts beyond the 1-5 day ranges typically captured by operational NWP.
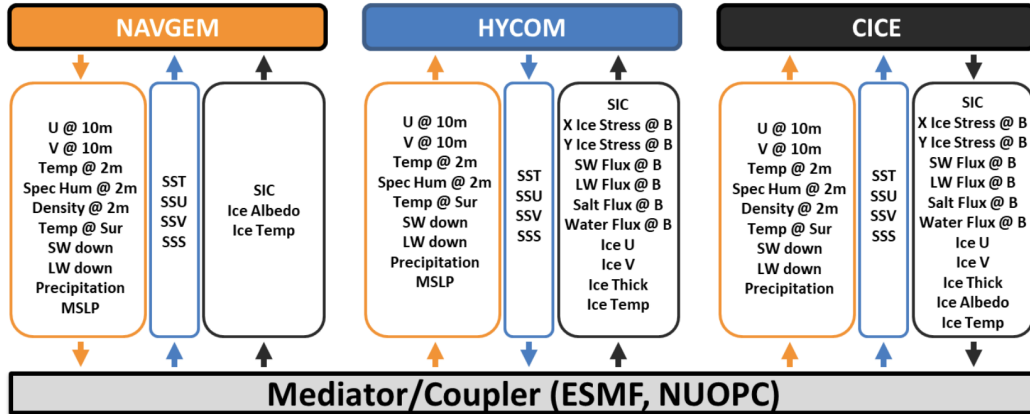
Figure 2.8. Model coupling schematic used by Navy ESPC and interactions between the three environmental models Image taken from Barton et al. (2019) with caption omitted.
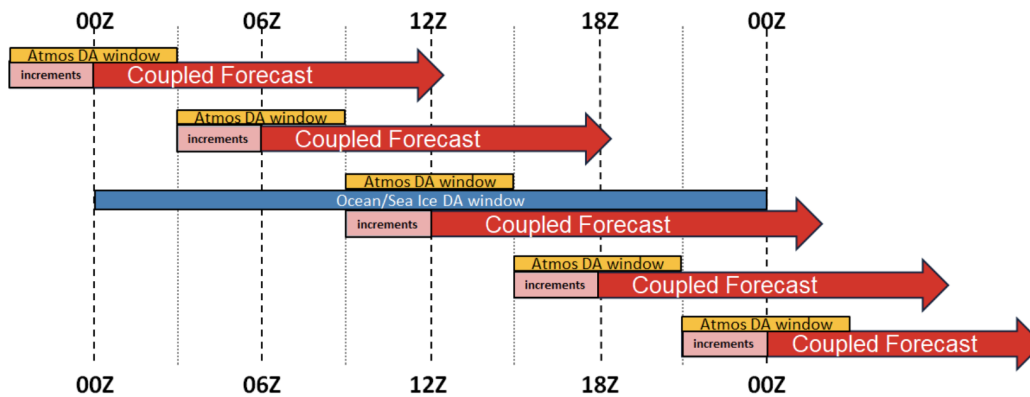
Figure 2.9. An explanation of how loosely coupled data assimilation is used in ESPC. Due to the differences in how atmospheric and ocean/ice data is assimilated, this approach allows the model to slowly account for feedback from the data without disturbing individual run times with new data. Image taken from Barton et al. (2019) with caption omitted.

For our study, in particular, the data available on the International Research Institute (IRI) platform for the purposes of the SubX project, had gaps of around three or four days where the model was not run nor was it able to assimilate new observations into older model runs. The website and project would take the last model run and advance the timeline that the last model projection indicated. As such, there are gaps in model data that exist in the amount of model runs that ESPC produced in this dataset but the total dataset is complete for all days during our study. Meaning that we have at least 41 days worth of forecast days for each model run and enough data to speak to the models tendencies but forfeit some quality in between runs due to some gaps that exist. It is worth noting that what is available from SubX is different from the operationalESPC forecasts, which started in August 2020, and consist of 16-member ensemble 45-day forecasts produced once per week.

CHAPTER 3:
Data and Methods

3.1   Data

To verify forecasts of Mistral events, the Lion Buoy, Station 61002, an observational buoy that is part of the National Data Buoy Center (NDBC) network at 42.102 N 4.703 E (42°6'9" N 4°42'9" E) off the coast of southern France and within the heart of the GOL is used. This buoy was operational from March 28, 2017 until October 1, 2018 and it recorded a myriad of atmospheric and oceanographic data. Within the data set, the wind direction and speed as well as significant wave height was recorded within the NDBC database at irregular intervals. An analysis of this data revealed that it was likely damaged by a Mistral. The last recording of the buoy in 2018 indicated a 35 knot wind from the northwest producing 18 ft seas and has since been nonoperational.

Given the limited time coverage of the Lion buoy, the logical and meteorological standard is to utilize reanalysis data that can provide an idealized substitute of environmental observations. The European Centre for Medium-Range Weather Forecasts (ECMWF) produces a set of ECMWF Reanalysis 5th Generation (ERA5) hourly data. Using this dataset spanning the August 5, 2017 - December 31, 2021 for wind speed and direction at the GOL buoy location as well as surface pressure, we captured the synoptic picture of the Mediterranean area. This ERA5 data revealed that of the 1610 days worth of daily averaged wind data, 273 days met the criteria of a Mistral event outlined in section 2.3. This gives us a standard rate of Mistral occurrence around 17% during the period of our study.

This method also provided a much more robust suite of data to work with than a single set of surface observations (Hersbach et al., 2020). In order to show that this ERA5 data does correlate to data with the NDBC Lion Buoy observations before substituting it for observations, Figure 3.1 below plots the reanalysis data against the observations over the dates that the buoy was operational. The plot shows that the reanalysis captures the buoy winds to within about +/- 5 kts. There is no consistent tendency to over or under analyze the winds and so the reanalysis data was used to verify all the model wind predictions.
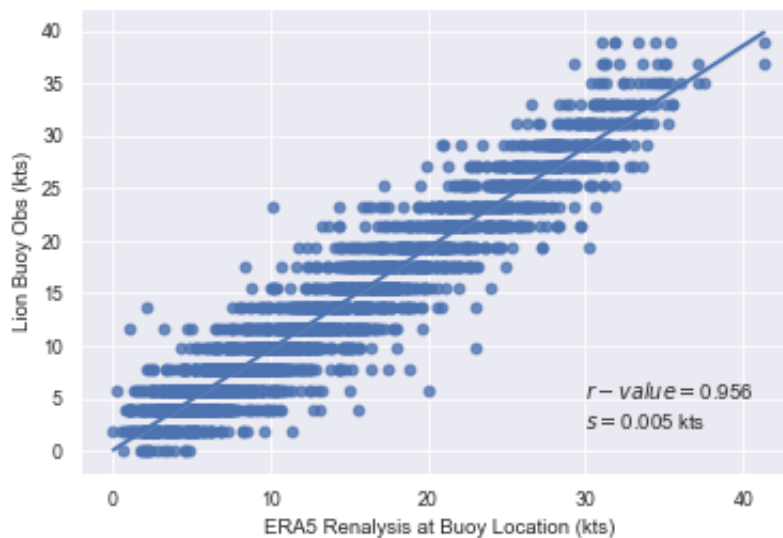
Figure 3.1. The regression plot between wind speed intensity of the ERA5 reanalysis data and the observed winds at the Lion Buoy Station 61002 from March 28,2017 - October 1, 2018

For the forecast data, a public library of ESPC data was available from the IRI Climate and Research Library. 45-day forecasts from the Navy ESPC system starting from four days each week are available through this SubX archive from 1999 through the present. The version of the ESPC model used for the SubX forecasts is very similar to the current version of ESPC that is run in operations as a 16 member ensemble run once per week starting in August 2020. On the SubX platform, the myriad of ESPC forecast and hindcast data is available and able to be downloaded into a Network Common Data File (netCDF). Using python code, we were able to organize the data into dataframes and compare values at the GOL buoy and locations pertinent to thumb rules using a package called pandas in order to conduct statistical analysis. In addition, we are able to create plots of the forecast and reanalysis data in order to gain a sense of the synoptic picture. This data will help us gain a sense of the model's inherent ability to forecast Mistral events as well as illustrate any added value when using forecaster thumb rules and synoptic pattern identification at the sub-seasonal time scale of ESPC.

3.2 Forecast Process

In order to accurately assess the capability of ESPC to detect the onset of a Mistral, the method that we used is multifaceted and includes data analysis methods and practical meteorological applications. The atmospheric component of ESPC is run at a 37-km resolution, which is lower resolution than many NWP models, and the output represents a daily average of a reduced 1x1 degree resolution. In order to explore the potential of useful forecasts beyond typical weather forecast timescales, the targeted forecast window that used was between 7-21 days. This also reflects a more practical sense of when an operational forecaster would most likely seek to use the ESPC model. By limiting the forecast window and using a year's worth of data, we were able to assess the model's ability to accurately forecast the Mistral over practical time periods while comparing enough data to show seasonal tendencies. The data was organized into seasons, by reviewing the solstice and equinox dates known over the years of data. Since model skill in representing and forecasting the oscillations such as the NAO, which impact Mistral events, varies by season, the data was analyzed as a function of season to aid in interpreting the results of the model and forecast process.

3.2.1 I: Quantitative Summary Analysis

To establish the baseline forecast skill for the ESPC model, forecast winds at the buoy location were verified by the wind analysis. This baseline was used to compare the impact of any added forecast criteria during further analysis. Using our criteria for a Mistral event (winds from 290°-345° at a minimum of 18 knots), we constructed a 2x2 Contingency Table to determine if an event was properly forecast using Roebber (2009) multiple measures method. This analysis computed the model's pure ability to forecast wind direction and wind speed within the GOL without additional criteria thus establishing the inherent ability of ESPC to correctly forecast Mistral wind events.

3.2.2 II: Applying Thumb Rules

Taking the data analysis idea further, we applied various intensity forecast thumb rules to the ESPC forecasts in order to see if one particular rule or a combination of these rules would improve the baseline skill established in part I. We ignore onset and cessation thumb rules as they are likely too small-scale and transient to be represented in averages of reanalysis and forecast data. The Brody and Nestor (1980) thumb rules are based on observations of

500 mb winds from Brest and Bordeaux, 850 mb winds from Nîmes, and surface pressure differences between Perpignan, Marseille, and Nice. Each of these thumb rules is derived from the synoptic flow pattern and observed conditions within the GOL. This analysis was done to determine if performing additional steps of other variables of ESPC forecast data will be a more or less predictable measure of Mistral onset conditions than the raw model output.

500mb winds at Brest and Bordeaux stations are what Brody and Nestor (1980) used to determine if the mid-level flow would support a katabatic wind into the GOL. Because ESPC SubX output includes 500 mb geopotential heights but not the forecast winds at that height, a simple conversion was needed to translate geopotential heights into geostrophic wind speed and direction at that pressure level. Using a May et al. (2022) package with the grid points closest to Brest and Bordeaux, we were able to convert the data into 500 mb winds and apply this rule as another predictive measure of the mistral in a contingency table.

The strongest correlation based on observed winds that Brody and Nestor (1980) found were the 850 mb winds at Nîmes. Using the zonal and meridional velocity variables at 850 mb on the grid point nearest to Nîmes, we are able to add this to the predictive measures that would imply the onset of a Mistral. Here, the relationship is notable based on the height of the observed winds and location of Nîmes relative to the GOL. This relationship is most likely a reason why Brody and Nestor (1980) found that it correlated with an r-score of .93 during their initial study. The nature of the wind coming from the north west of the GOL combined with the level appropriate to see the highest winds, makes this the preferred forecast rule for the authors when it was published.

Finally, the surface pressure spread from the grid points near Perpignan, Marseille, and Nice was analyzed using the surface pressure grid points nearest to the three locations. The intensity thumb rule states that a 6 mb spread at the surface between the stations of Perpignan and Nice or a 3 mb spread between any of the stations is indicative of a closed low pressure system over Genoa, Italy. This low pressure system would tighten the gradient winds between that low pressure system and the Azores high pressure system to the west. Unfortunately, this is only a good thumb rule for a type B Mistral based on the Brody and Nestor (1980) synoptic setup.

The purpose of adding these three thumb rules, whether used separately or in combination, is to show whether added measures would improve forecast quality based on the step I baseline. Because the thumb rules are based in physical relationships between the observation stations and conditions in the GOL, the hope is to show that the rules highlight another relationship between the forecast data and observed Mistral events and increase the skill.

3.2.3   III: Practical Application

Forecasting can be described as an art based on a science. Often operational forecasters analyze synoptic patterns to get a keen sense of the overall forces of the environment being presented. The differences between model runs in NWP are often graphical displays of statistical trends that the model is computing over the several iterations. In order to minimize error, forecasters utilize ensemble models to show how model forecasts may diverge when starting from slightly different initial states, representing uncertainty in the analyses. As we do not have "true" Navy ESPC ensembles available to us through the SubX archive, we can create an "ensemble of opportunity", or time-lagged ensemble, by seeing how the forecasts started from different dates diverge from each other. We study this sensitivity to the initial state by comparing forecasts that are valid at the same time, but were run from analyses valid on different days and weeks prior to a known event. We analyze the synoptic features forecast by ESPC and compare that against the reanalysis data valid at the time of the event. By doing so, we can show a graphical timeline of what ESPC can provide to a forecaster in the weeks leading up to an event by assuming that an event would have impacted their operations. This will give us a more practical sense of how an operational forecaster can utilize days of ESPC model runs much like an ensemble model would show iterations of the same system.
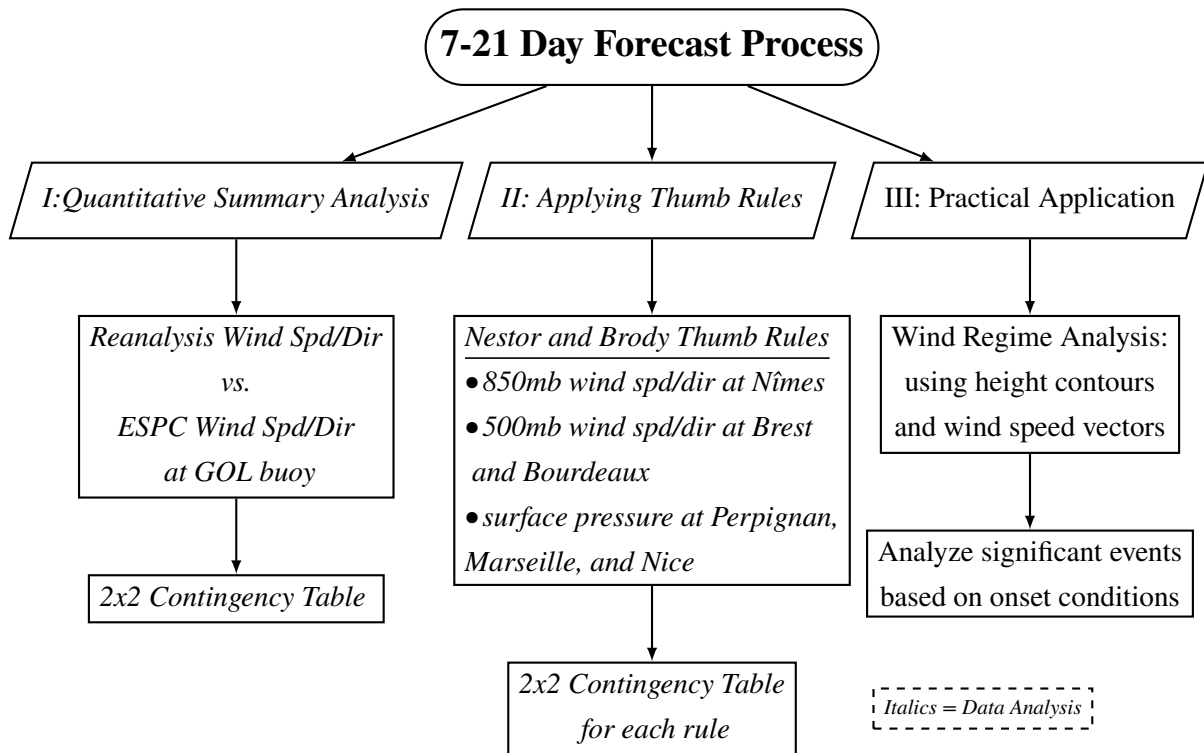
Figure 3.2. Using Brody and Nestor (1980) rules and idealized forecast window of 7-21 Days before the onset of a Mistral wind event. This process should give hard data points related to onset as well as apply meteorological reasoning in a practical sense within the targeted forecast window

3.3   Measuring Forecast Quality

In order to evaluate the ability of ESPC to forecast Mistral events, we will utilize the methods of Roebber (2009) and construct a 2x2 Contingency Table for Steps I and II (see example table 3.1 below). Where 'A' represents the number of properly forecast days for an observed Mistral event based on our criteria in Section 2.3 ("Hits"), 'B' represents the number of forecasts for Mistral event days that did not occur based on reanalysis ("False Alarms"), 'C' represents forecasts for Mistral events that did occur based on reanalysis but were not forecast to occur ("Misses"), and 'D' is the correct number of forecast non-Mistral days where an event did not occur ("Correct Nulls"). Using these metrics, we were able to assign

values to the model's ability to correctly identify instances in which the Mistral was likely as well as unlikely based on numerical model output and impacts from seasonal oscillations.

2x2 Contingency Table		Event Observed	
		Yes	No
Event Forecast	Yes	A	B
	No	C	D

Table 3.1. Sample 2x2 Contingency Table for establishing measured forecast quality: Using established criteria of a particular forecast metric (rain, fog, tornado, etc.), you can assess the accuracy of a model to predict events based on a test of whether or not the event occurred and whether it was forecast to occur. The table then produces a count of these logical tests and the counts are designated as variables A, B, C, and D. These variables are calculated and used to determine of accuracy of the model or process used to forecast the event (Roebber, 2009).

The Probability of Detection (POD) gives us a measure of how successful the test was at predicting the event between 0 and 1. It is calculated by taking:

$$\text{POD} = \frac{A}{A + C} \tag{3.1}$$

The False Alarm Ratio (FAR) gives an indication of how often the model predicts an event to occur mistakenly (Success Ratio (SR) = 1−FAR) and is calculated by:

$$\text{FAR} = \frac{B}{A + B} \tag{3.2}$$

Finally, the Critical Success Index (CSI) is a metric combining the previous two that can be analyzed to indicate the likelihood of the event occurring given the inherent ability of the POD and FAR and is calculated by this equation:

$$\text{CSI} = \frac{A}{A + B + C} \tag{3.3}$$

3.4   Methods Summary

By using the ERA5 reanalysis data to substitute for observations and the ESPC model data parameters, we have created an aggregate of what an operational forecaster would have at his/her disposal to forecast the onset of a Mistral. As such, we are able to assess whether or not ESPC is able to inherently forecast Mistral events, the utilization of thumb rules created for short term forecast windows can be used to increase forecast accuracy, or if there is utility in synoptically observing changes in forecast data from daily forecasts in order to assess the likelihood of a Mistral. By investigating with these three methods, we can assess the model's ability to project seasonal impacts to the area and thereby observe the accuracy of ESPC to aide in the forecast of the Mistral wind event in the S2S time scale.

CHAPTER 4:
Results

4.1 I: Quantitative Summary Analysis Results

Looking at raw model forecast output can be an indication of the inherent skill of the forecast model to predict the conditions of the environment. Using just the model wind forecasts and no additional forecast metrics or thumb rules establishes a baseline that is compared in future tests to show an improvement or deterioration of skill by adding the additional forecast criteria. Here, we see ESPC's inherent ability to forecast the Mistral winds at the GOL buoy location in the contingency table (Table 4.1) as well as radial plots comparing wind forecasts to reanalysis data for all forecasts (Figs. 4.1, 4.3, and 4.2) as well as Mistral event forecasts (Figs. 4.4. 4.6, and 4.2). These numbers and plots provided a baseline to enable comparisons of Step II forecast thumb rules to show marginal improvement by applying additional thumb rule criteria.

ESPC Surface Winds at GOL Buoy		Event Observed		POD	.108
				FAR	.800
		Yes	No	SR	.200
Event Forecast	Yes	249	996	bias	.5390
	No	2061	10326	CSI	.0753

Table 4.1. This table shows the ESPC 7-21 day forecast wind data when predicting Mistral conditions at the GOL buoy location from August 5th, 2017 to December 31st.

ESPC Surface Winds at GOL Buoy (14-21 Day Forecast)		Event Observed		POD	.091
				FAR	.827
		Yes	No	SR	.173
Event Forecast	Yes	113	539	bias	.5262
	No	1126	5476	CSI	.0636

Table 4.2. This table shows the ESPC 14-21 day forecast wind data when predicting Mistral conditions at the GOL buoy location from August 5th, 2017 to December 31st.

ESPC Surface Winds at GOL Buoy (7-14 Day Forecast)		Event Observed		POD	.120
				FAR	.776
		Yes	No	SR	.224
Event Forecast	Yes	149	515	bias	.5346
	No	1093	5529	CSI	.0848

Table 4.3. This table shows the ESPC 7-14 day forecast wind data when predicting Mistral conditions at the GOL buoy location from August 5th, 2017 to December 31st.

From these contingency tables, we can see an increasing amount of skill as we decrease the forecast time to seven days. There are interesting numbers to highlight here such as ESPC forecasts Mistral events about half as many times than they actually occur. That ratio holds true on each of the time frames between the 7-21, 14-21, and 7-14 day forecasts. We can conclude that based on the relative number of misses (event observed but not forecast to occur) and false alarms (event forecast to occur but did not occur). Also, the amount of correct nulls (not forecast to occur and did not occur) stays relatively the same in the smaller forecast windows. This means that the model does show some skill but not that above climatology where Mistral events occurred around 17% of the time (273 events in 1610 days between August 5th, 2017 and December 31st)
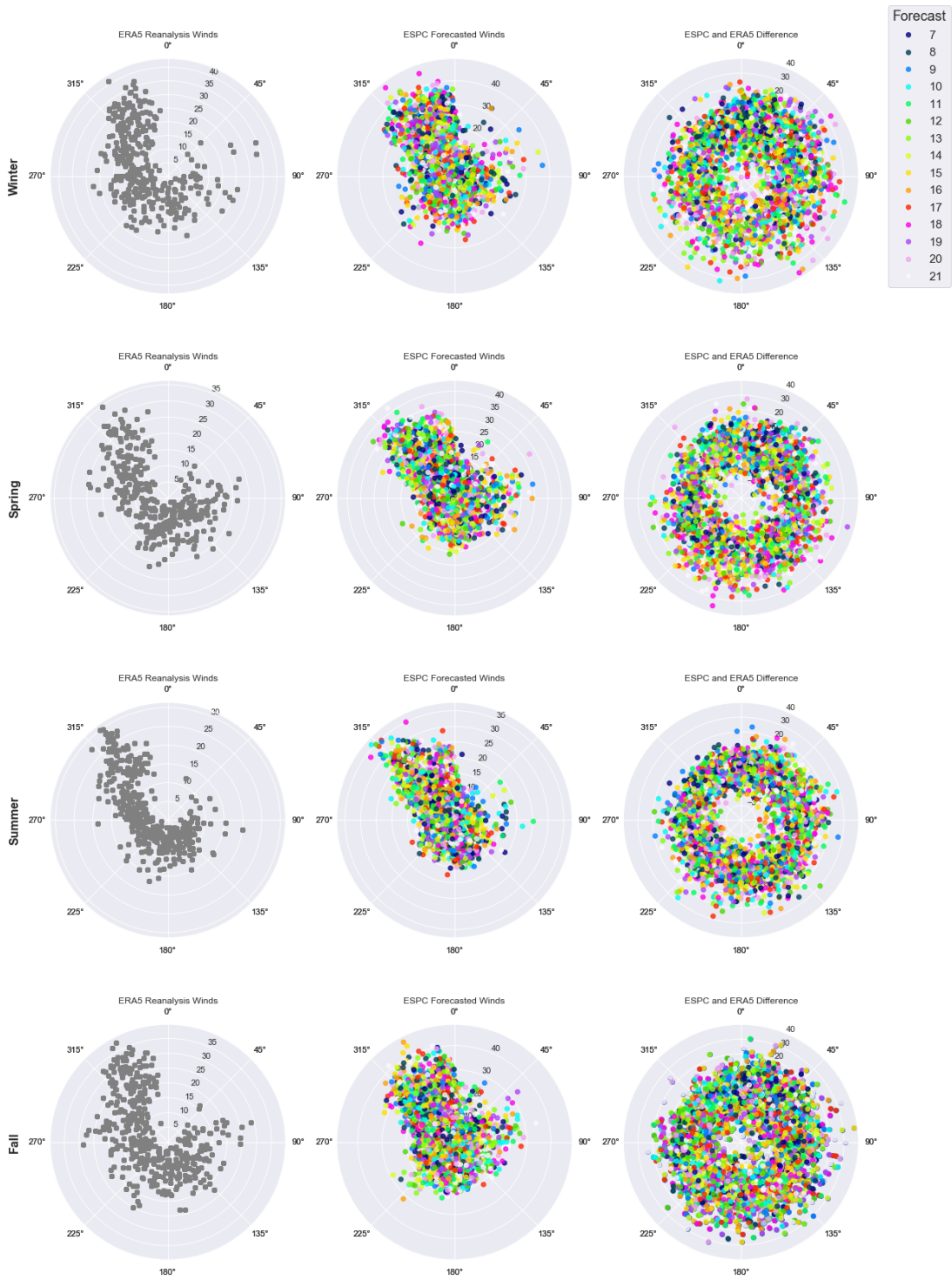
Figure 4.1. ERA5 reanalysis winds and ESPC forecast winds for August 5th, 2017 to December 31st plotted by season in the 7-21 forecast time frame.

Figure 4.2. ERA5 reanalysis winds and ESPC forecast winds for August 5th, 2017 to December 31st plotted by season in the 14-21 day forecast time frame.

Figure 4.3. ERA5 reanalysis winds and ESPC forecast winds for August 5th, 2017 to December 31st plotted by season in the 7-14 forecast time frame.
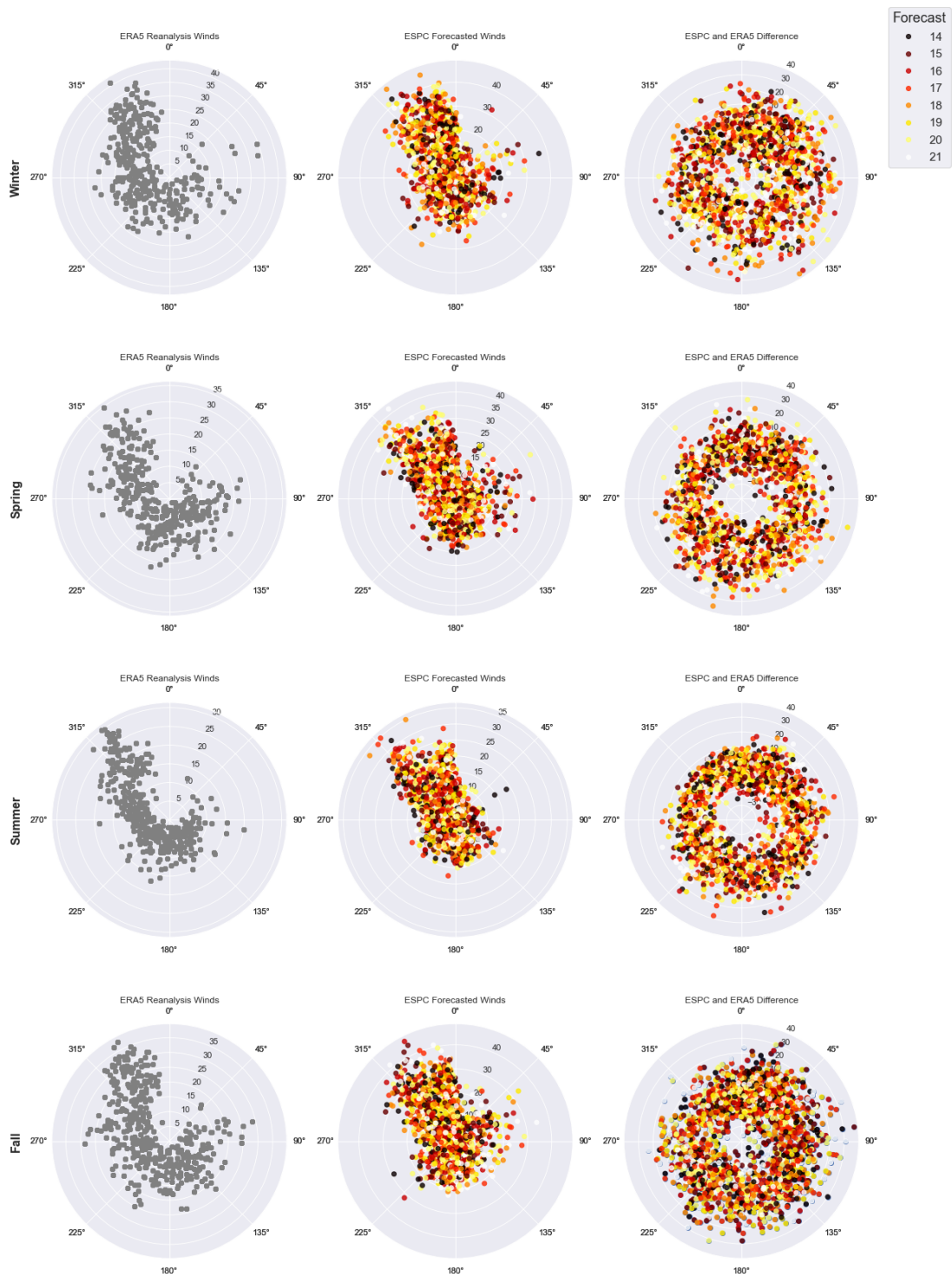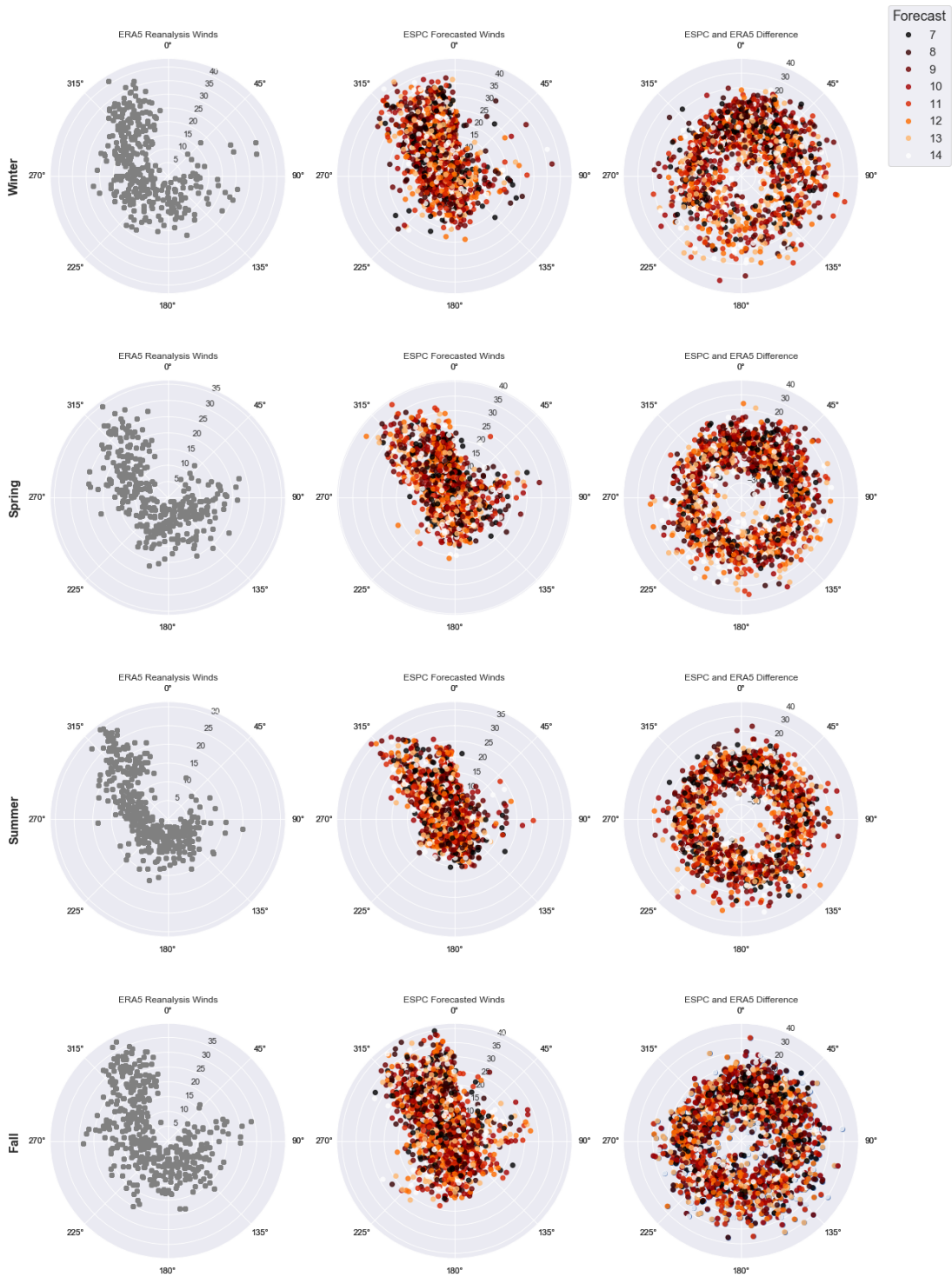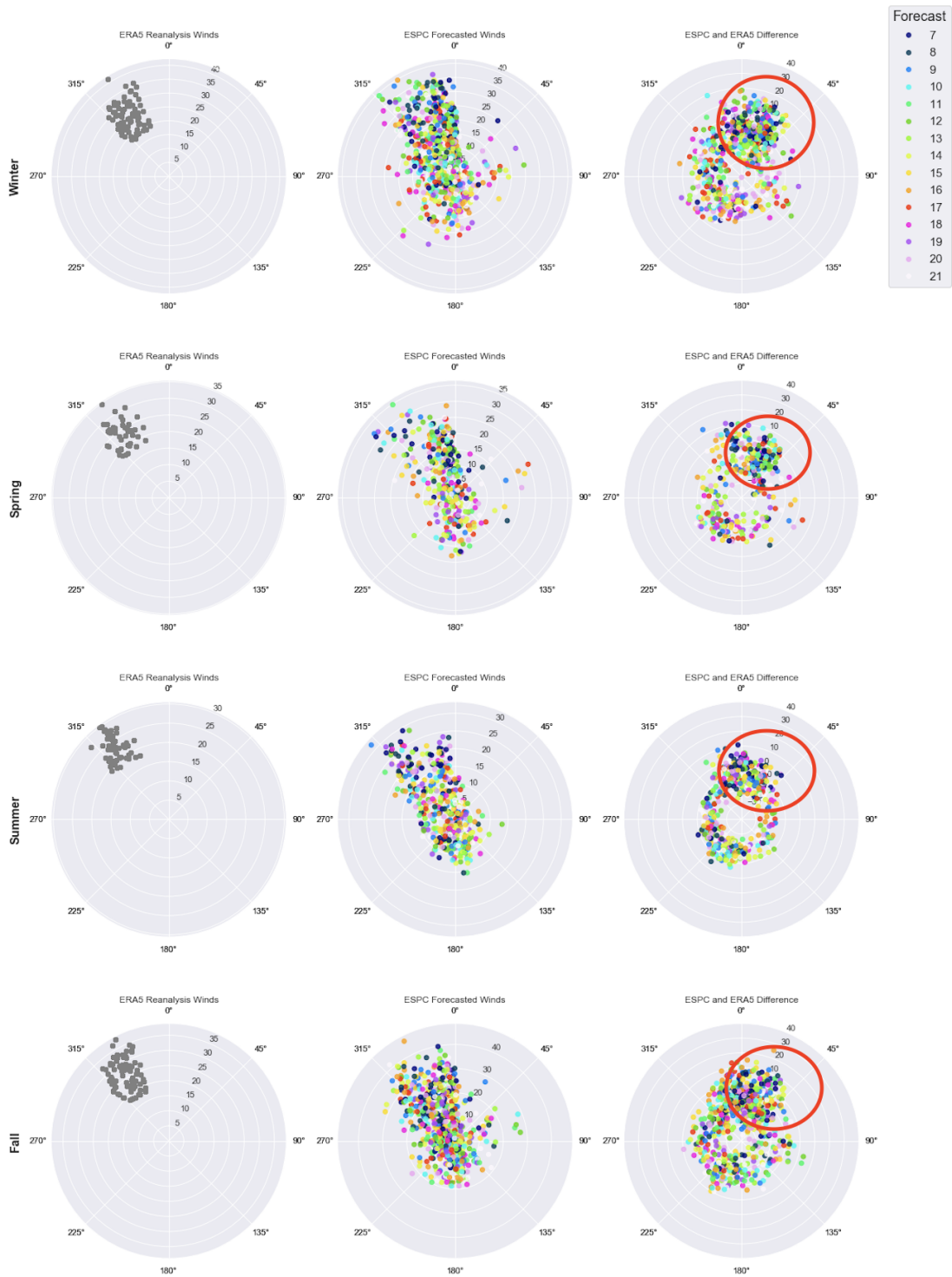
Figure 4.4. ERA5 Mistral event reanalysis winds and ESPC forecast winds for August 5th, 2017 to December 31st plotted by season in the 7-21 forecast time frame.
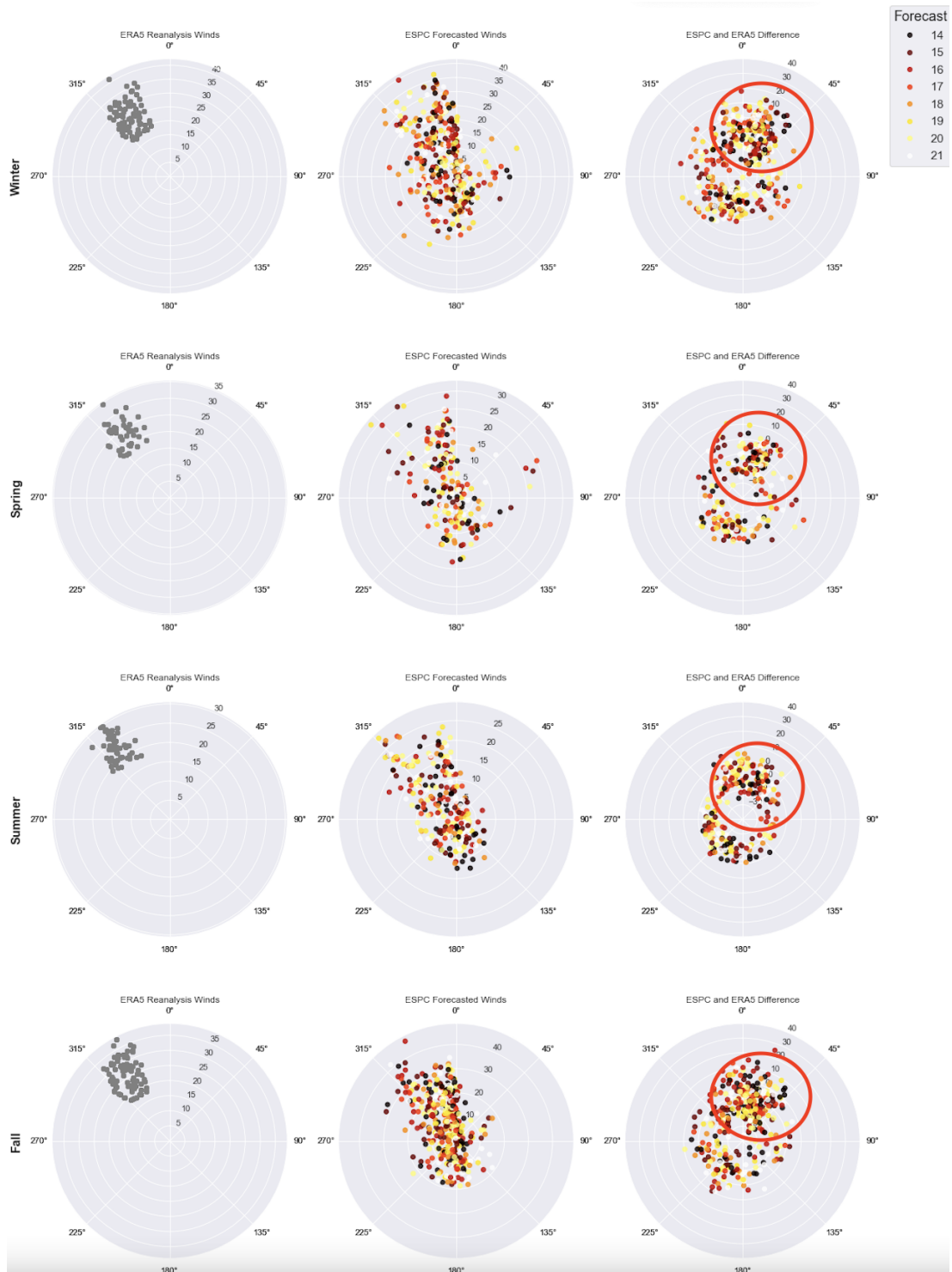
Figure 4.5. ERA5 Mistral event reanalysis winds and ESPC forecast winds for August 5th, 2017 to December 31st, 2021 plotted by season in the 14-21 forecast time frame.
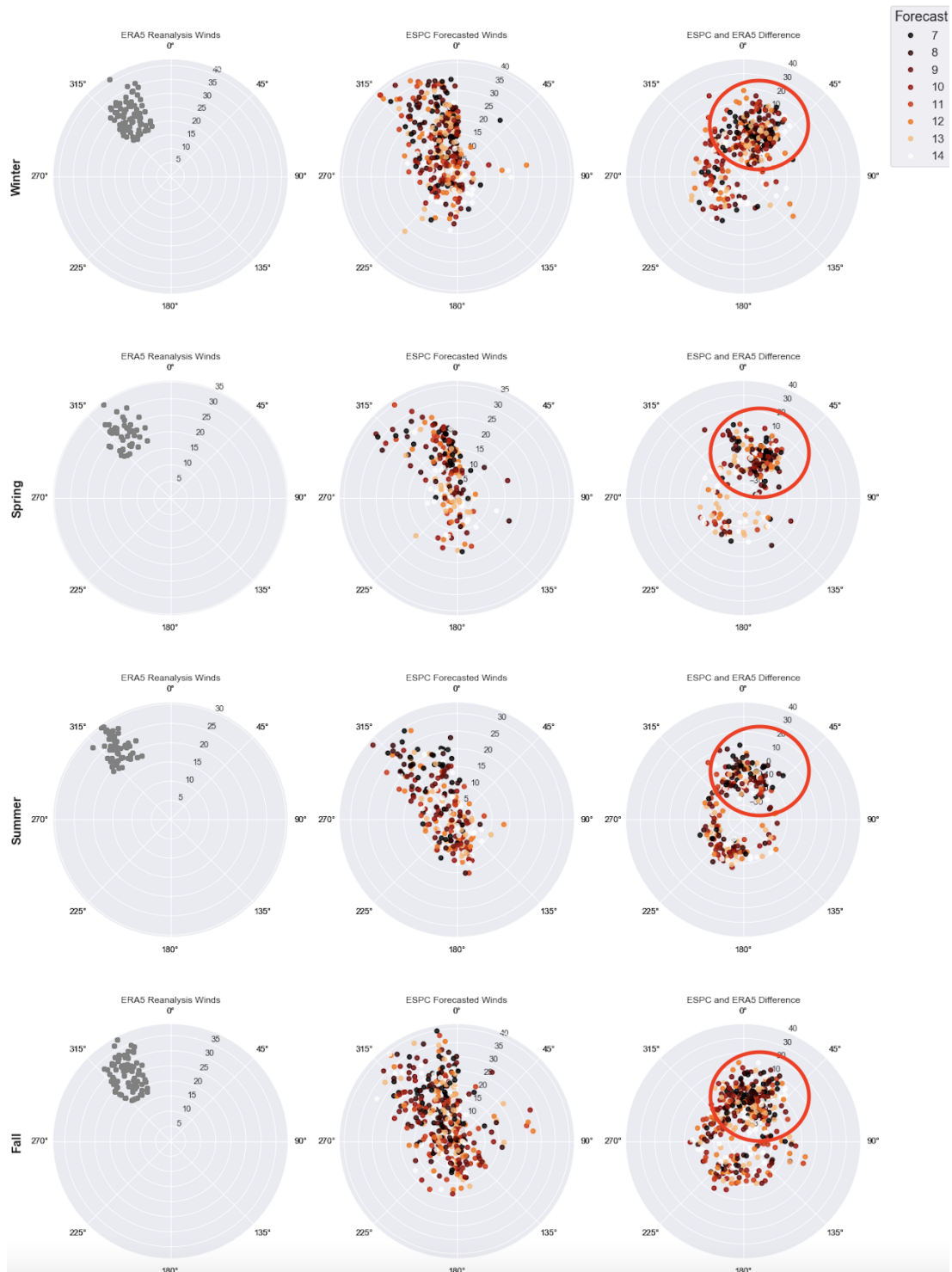
Figure 4.6. ERA5 Mistral winds and ESPC forecast winds plotted by season in the 7-14 forecast time frame.

The seasonal plots show in 4.1 display a typical distribution of winds and wind error from the ERA5 and ESPC plots done by season. The plots on the right show the difference between the reanalysis and forecast wind data. The intersection of zero error for direction and intensity is the in the "12 o'clock and middle" portion of the plot. There is no discernible trend towards the intersection of zero error that is apparent in these plots. Plots illustrate the difficulty in locating a bias in the seasons or any trends that the forecast model is producing beyond a typical distribution of error in both wind and direction. There does, however, appear to be a slight trend for smaller error during the summer where both wind speed and directional error are smaller when compared to the other seasons.

When split into forecast periods of 7-14 and 14-21 day plots in 4.3 and 4.2 there is a slight tendency for the 7-14 day data to trend towards the zero error intersection. The overall forecast error in Fig. 4.3 for 7-14 days over all seasons is less than the error in Fig. 4.2 for the 14-21 day forecasts. These plots of raw model winds compared to reanalysis winds in a reduced time frame illustrate the difficulty the model has in forecasting wind direction and intensity on these multi-week timescales.

Fig. 4.4 shows the isolated Mistral events relevant to our study. Within these plots, a definite trend towards the zero error origin is evident, most notably in the winter error plot. From this figure, we can also notice a tendency for the longer forecast runs to under-forecast the intensity and reduce the error as the forecast time approaches the 7-day mark. It is also worth noting that the fall season has the tightest grouping near the zero error intersection while also having the most darker marks in the lower half of the radial plot indicating a greater amount of error at the shorter forecast periods relative to other seasons.

When broken down into separate 7-14 and 14-21 day plots, as shown in 4.5 and 4.6, the data shows further evidence that the model forecasts intensity correctly but tends to be to the right for wind direction. The "just to the right" error shown in these plots is indicative of a bias within the forecast model and around 15-25° of directional error.

In summary, the raw wind forecast model data show a typical error pattern in our forecast window for all wind data during the five years of data we analyzed. However, when we isolated the events studied to known Mistral events, the shorter forecast periods did display skill with intensity while showing slight error to the right for wind direction. These plots

show that when Mistral wind events occur, ESPC displays a higher level of skill when compared to wind forecasts from all directions and intensities.

4.2   II: Applying Thumb Rules

Each forecast thumb rule represents an intensity thumb rule from Brody and Nestor (1980). The ERA5 data was run to test the inherent skill of the thumb rule before testing the ability of ESPC to forecast based on the same parameters as the thumb rule. What we'd like to see is a marked improvement of the accuracy in the POD and CSI calculations without increasing the FAR.

4.2.1   Nîmes 850 mb Thumb Rule

ERA5 Nîmes 850 mb Thumb Rule Test		Event Observed			
				POD	.187
		Yes	No	FAR	.393
Event Forecast	Yes	51	33	SR	.607
	No	222	1304	CSI	.1667

Table 4.4. This table shows the ERA5 reanalysis data using the Nîmes 850 mb forecast thumb rule for Mistral events from August 5th, 2017 - December 31st, 2021. Thumb rules used were: 850 mb winds from 330°-010° or 340°-020° and at least 50 kts.

ESPC Forecast Using Nîmes 850 mb Winds Thumb Rule		Event Observed		POD	.287
		Yes	No	FAR	.761
Event Forecast	Yes	838	2671	SR	.239
	No	2086	7917	CSI	.1498

Table 4.5. This table shows the ESPC 7-21 day forecast data using the Nîmes 850 mb thumb rule for Mistral events from August 5th, 2017 to December 31st. Thumb rules used were: 850 mb winds from 330°-010° or 340°-020° and at least 50 kts.

Here, the Nîmes thumb rule was applied to the ERA5 analyses (Table 4.4) and ESPC forecasts (Table 4.5). This Nîmes 850 mb thumb rule does not show a reliable predictive measure of Mistral events for either the ERA5 analyses nor the ESPC forecasts. The ESPC forecasts are slightly improved compared to the direct wind forecasts (Table 4.1). There's a marginal gain made in POD but it is also accompanied by a gain in FAR and decrease in SR. This leads me to believe that the ESPC model shows a tendency to forecast northerly winds and might be due to a bias towards climatology for Mistral events and not necessarily a predictive measure that we should consider.

4.2.2 Brest and Bordeaux 500 mb Thumb Rule

ERA5 Brest and Bordeaux 500 mb Thumb Rule Test		Event Observed		POD	.062
		Yes	No	FAR	.514
Event Forecast	Yes	17	18	SR	.486
	No	256	1319	CSI	.0584

Table 4.6. This table shows the ERA5 reanalysis data using the Brest 500mb and Bordeaux 500 mb forecast thumb rules for Mistral events from August 5th, 2017 to December 31st. Thumb rules used were: 500 mb winds from 295°-345° at least 65 kts from either station.

ESPC Forecast Using Brest and Bordeaux 500 mb Thumb Rules	Event Observed				
			POD	.024
	Yes	No	FAR	.757
Event Forecast	Yes	54	168	SR	.243
	No	2232	11058	CSI	.022

Table 4.7. This table shows the ESPC 7-21 forecast data using the Brest 500 mb and Bordeaux 500 mb forecast thumb rules for Mistral events from August 5th, 2017 to December 31st. Thumb rules used were: 500 mb winds from 295°-345° at least 65 kts from either station.

Interestingly enough, this was the thumb rule that I had largely anticipated would be the most accurate predictor and it was very much not a reliable thumb rule. Neither the ERA5 (Table 4.6) nor the ESPC forecasts (Table 4.7) show much skill with the PODs very low and well below the direct model wind forecasts (Table 4.1). When using this thumb rule, Brody and Nestor (1980) had two rules, onset and intensity, both were included in this test but neither materialized into a reliable measure of prediction. The possibility of error in the tests were examined and I considered the calculations made to get the geopotential height into geostrophic winds but an obvious error was not identified. My conclusion is simply that during the analysis of data that Brody and Nestor (1980) inventoried this must have been a rule that had minimal data to support or an error in observational data may have been the cause. This also leads me to question the authenticity of some of the other thumb rules as indicators of events and suggests that maybe they tend toward being convenient observations made through the lens of the forecaster.

4.2.3 Surface Pressure Spread Between Perpignan, Marseille, and Nice Thumb Rule

ERA5 Surface Pressure Spread at Perpignan, Marseille and Nice Thumb Rule		Event Observed			
				POD	.424
		Yes	No	FAR	.837
Event Forecast	Yes	103	527	SR	.163
	No	140	624	CSI	.1338

Table 4.8. This table shows the ERA5 reanalysis data using the surface pressure spread thumb rule between Perpignan, Marseille, and Nice for Mistral events from August 5th, 2017 to December 31st. Thumb rules used were: at least 6 mb of difference between Perpignan and Nice or 3mb of difference between any of the stations

ESPC Surface Pressure Spread at Perpignan, Marseille, and Nice Thumb Rule		Event Observed			
				POD	.584
		Yes	No	FAR	.813
Event Forecast	Yes	1336	5790	SR	.187
	No	950	5436	CSI	.1654

Table 4.9. This table shows the ESPC forecast data using the surface pressure spread thumb rule between Perpignan, Marseille, and Nice for Mistral events from August 5th, 2017 to December 31st. Thumb rules used were: at least 6 mb of difference between Perpignan and Nice or 3 mb of difference between any of the stations

Looking at the ERA5 data (Table 4.8), it is clear that this thumb rule has some legitimate ability as a predictor of Mistral events. The mb spread is most likely present during each type due to either leeside troughing from the upstream winds or indicative of a closed low pressure system that experienced genesis from the lee of the mountains. Either way, it seems

as an example of where a thumb rule was both dynamically correct and a reliable predictor of Mistral events. The gain of POD by about 16% was made by ESPC to correctly forecast events based on the results shown in Fig. 4.1. Additionally, the FAR and SR were nearly identical to the reanalysis winds at the GOL buoy location. This suggests that the rule is effective within the ESPC model as an indication of a Mistral event. The FAR, we believe, is due to a naturally occurring leeside trough that is present when the upstream winds begin to approach the French Alps. Although the troughing and natural lower pressure may be always present the spread in the locations mentioned in the thumb rule help put into context the connection between the deepening and widening of that troughing and the likelihood for Mistral events to occur.

4.2.4   All Thumb Rules

ERA5 All Thumb Rules		Event Observed			
				POD	.462
		Yes	No	FAR	.811
Event Forecast	Yes	126	541	SR	.189
	No	147	796	CSI	.1548

Table 4.10. This table shows the ERA5 reanalysis data using all forecast thumb rules for Mistral events from August 5th, 2017 to December 31st. Thumb rules used were: 850 mb winds from 330°-010° or 340°-020° and at least 50 kts, 500 mb winds from 295°-345° at least 65 kts from either station, or at least 6 mb of difference between Perpignan and Nice or 3 mb of difference between any of the stations

ESPC All Thumb Rule Forecast		Event Observed		POD	.474
		Yes	No	FAR	.819
Event Forecast	Yes	1477	6672	SR	.181
	No	1641	8229	CSI	.1509

Table 4.11. This table shows the ESPC forecast data using all forecast thumb rules for Mistral events from August 5th, 2017 to December 31st. Thumb rules used were: 850 mb winds from 330°-010° or 340°-020° and at least 50 kts, 500 mb winds from 295°-345° at least 65 kts from either station, or at least 6 mb of difference between Perpignan and Nice or 3 mb of difference between any of the stations

4.3 III: Practical Application

Here, the objective is use ESPC forecast data leading up to a known Mistral event based on our criteria found in our ERA5 dataset. I identified known Mistral events lasting one, three, and five days. These criteria were the same used in the previous sections but meant to show the deterministic forecast of the synoptic picture that a forecaster would be presented with when looking for Mistral events. In order to display the reanalysis and forecast plots, we utilized a Cartopy python package (Met Office, 2010 - 2015).

4.3.1 Mistral Event: June 13-18, 2018
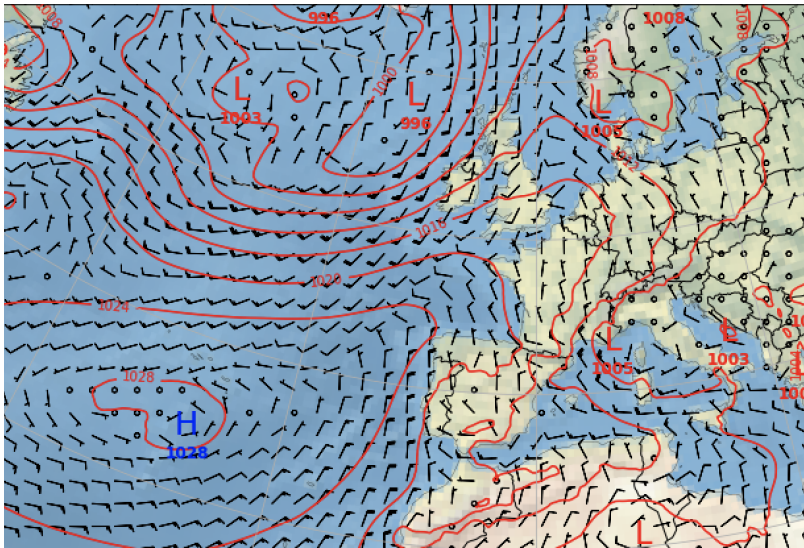
Figure 4.7. ERA5 reanalysis plot for 06-13-2018.
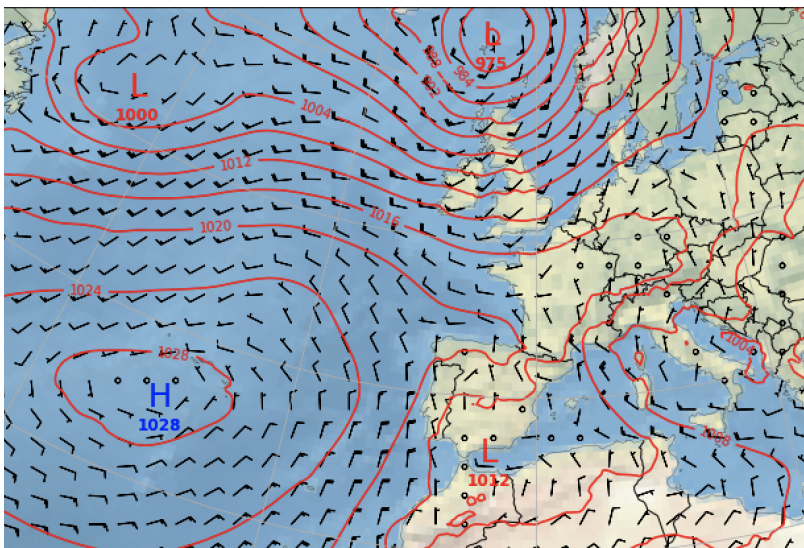

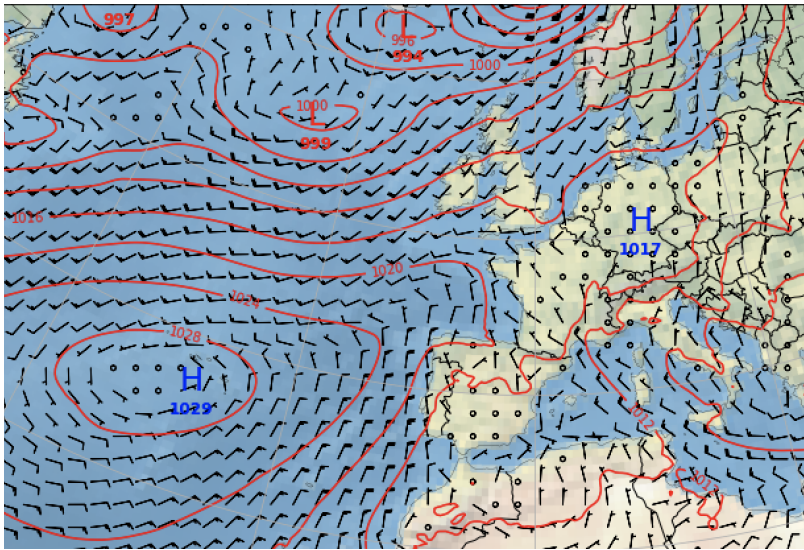Figure 4.8. ERA5 reanalysis plot for 06-14-2018.

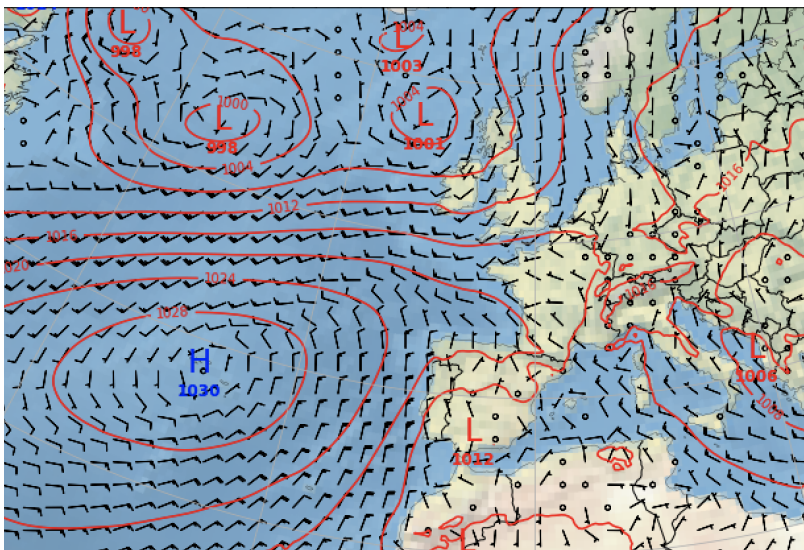Figure 4.9. ERA5 reanalysis plot for 06-15-2018.

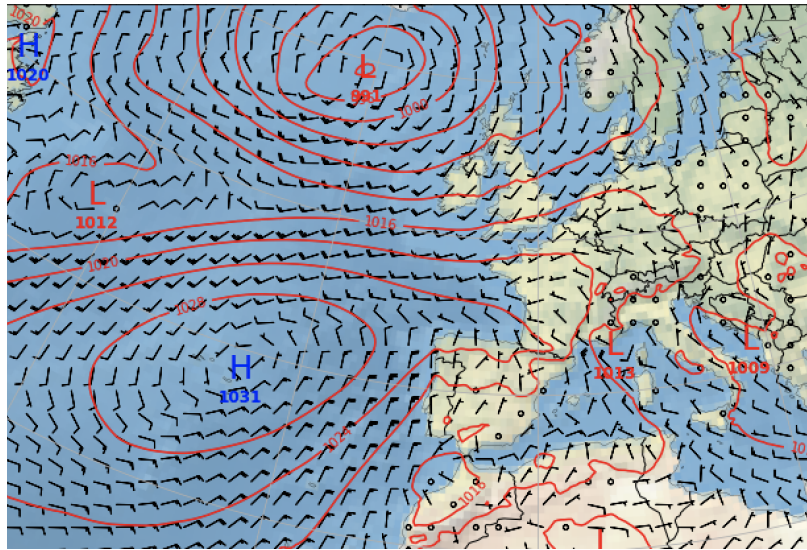Figure 4.10. ERA5 reanalysis plot for 06-16-2018.

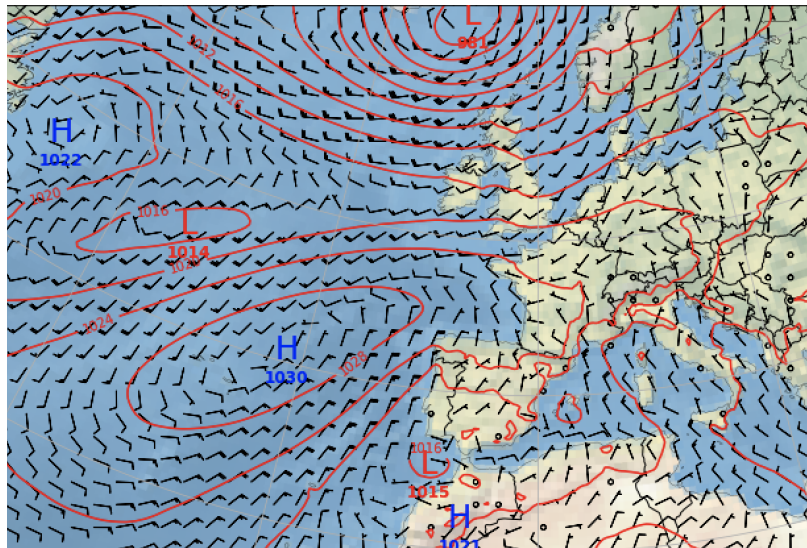Figure 4.11. ERA5 reanalysis plot for 06-17-2018.

Figure 4.12. ERA5 reanalysis plot for 06-18-2018.

This event, shown in Figs. 4.7-4.12, represents an anomalously long Mistral event that occurred for six days where winds reached an average of over 25 kts slightly northwest from the GOL buoy location. A series of low pressure systems were located in the North Atlantic and tightened the gradient between the Azores high pressure system. This caused

strong zonal winds to enter the Bay of Biscay before taking a more meridional path into the GOL where the ridging from the Azores high forced winds into Carcassone Gap and Rhône Valley. Given the time of the year in which this event occurred, the error plots from Fig. 4.4 suggests that the model is able to identify the wind speed and direction during the event within the forecast window with skill.

Analysis was conducted on all ESPC forecasts plots valid during this six day event. For the sake of brevity, we will target the strongest Mistral day, in this case, 06-15-2018 shown in Fig. 4.9, and analyze all forecast plots available from 21 days ahead of the event until 7 days ahead where a global forecast NWP model is more appropriate. As noted, in Section 2.6, gaps exist in between model runs due to the experimental nature of ESPC at the time when it was produced. Therefore, we will display the strongest day of the period in order to show the model forecasts for that day only instead of all the model forecasts that were valid during that entire event.
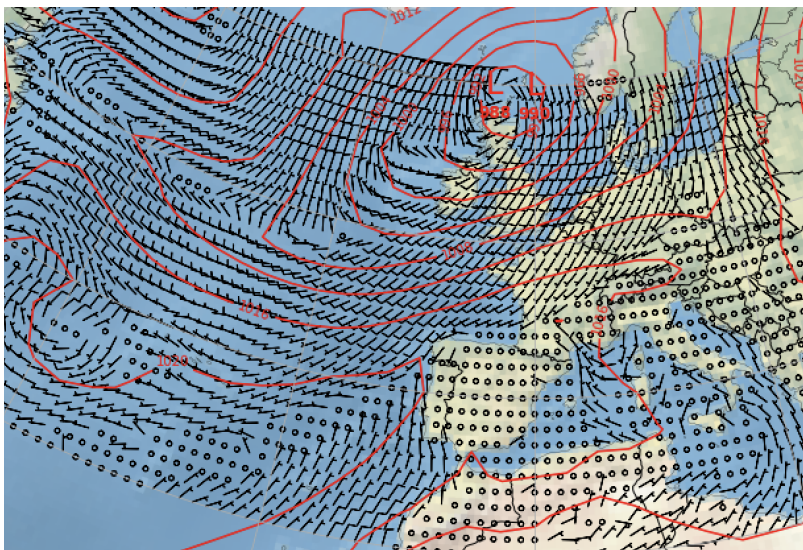

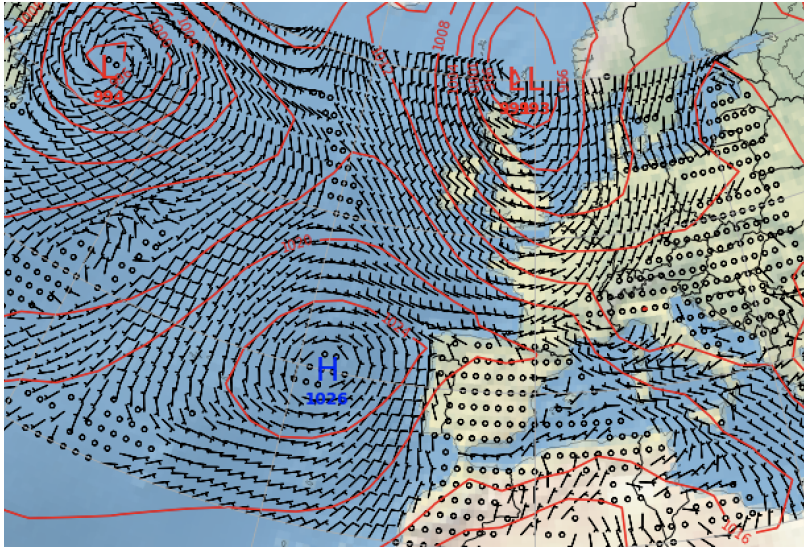Figure 4.13. ESPC forecast plot for 06-15-2018 produced on 05-27-2018

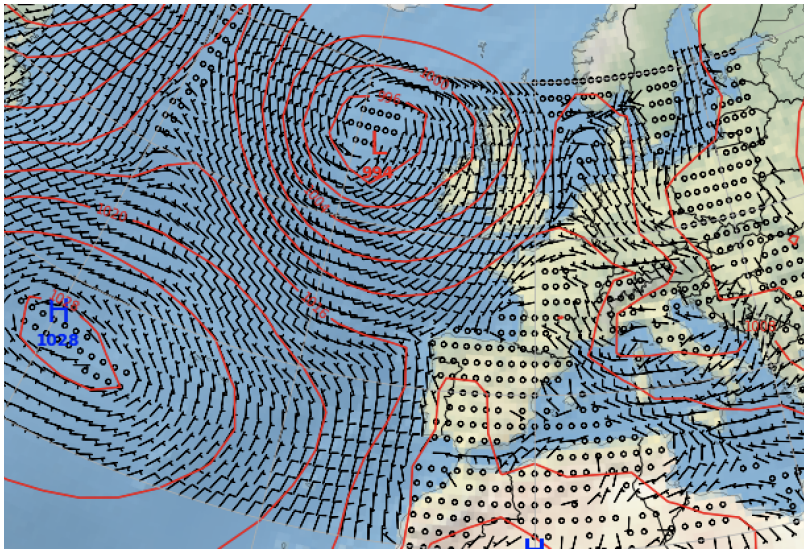Figure 4.14. ESPC forecast plot for 06-15-2018 produced on 05-28-2018

Figure 4.15. ESPC forecast plot for 06-15-2018 produced on 06-02-2018
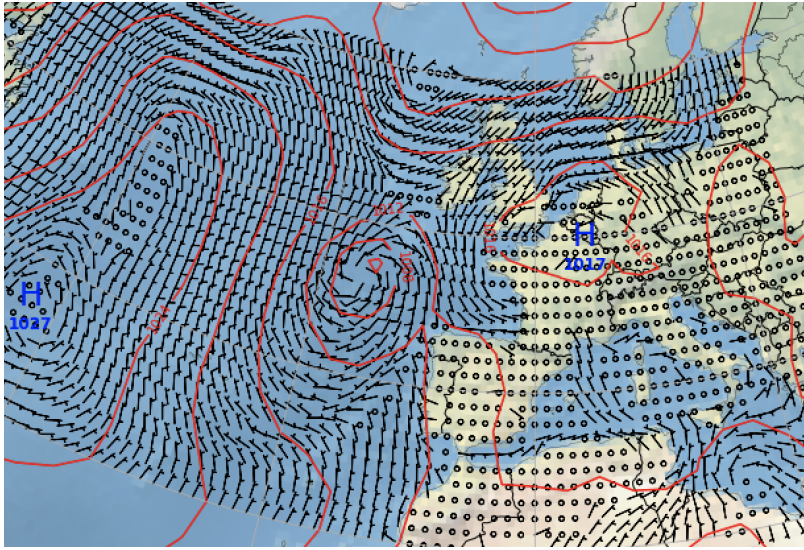
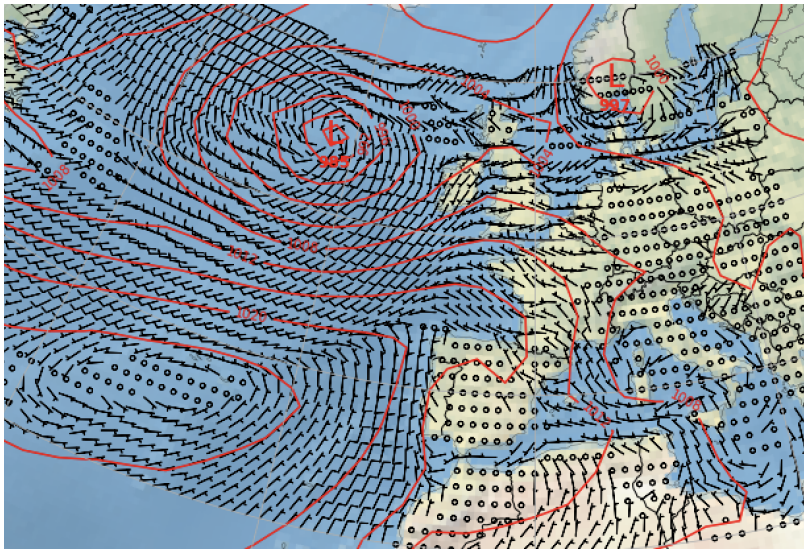Figure 4.16. ESPC forecast plot for 06-15-2018 produced on 06-03-2018

Figure 4.17. ESPC forecast plot for 06-15-2018 produced on 06-04-2018
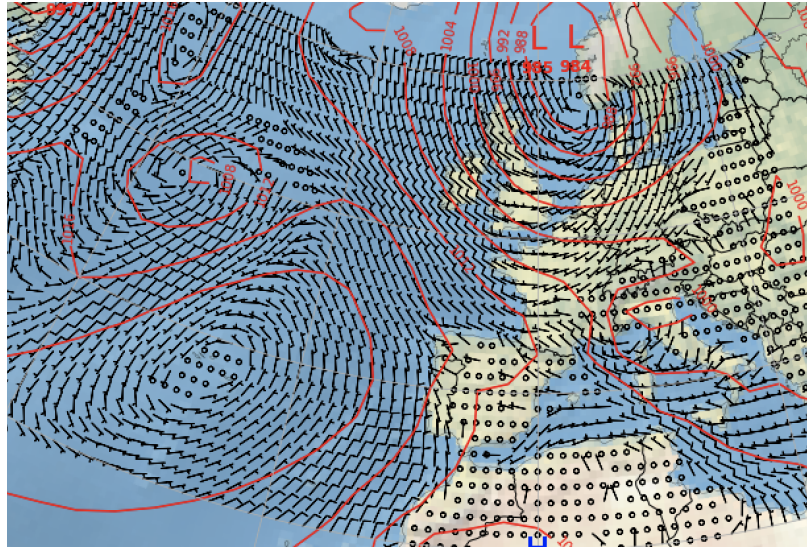
Figure 4.18. ESPC forecast plot for 06-15-2018 produced on 06-05-2018

In this series of plots, all valid on 06-15-2018, we begin by looking at Fig. 4.13 and see indications of northwesterly flow in the GOL. Frontal winds extend behind the implied cold front on the system in the North Sea but ridging from the mid-Atlantic high is not well identified and confused winds over most of the Iberian Peninsula offer little evidence that anti-cyclonic flow is entering the gaps needed to induce a Mistral. In Fig. 4.14 the ridging and associated anti-cyclonic flow is shown and a gradient is apparent between the aforementioned low from Fig. 4.13. In Fig. 4.15 northwesterly flow remains apparent in the GOL but might be better attributed to pre-frontal winds from the cold front associated with the low pressure system west-northwest of Ireland in the North Atlantic. Here, moving the location of the low pressure system still has induced Mistral condition but not due to the synoptic setup described in Fig. 4.9. In Fig. 4.16, a cut-off low pressure system, located northwest of the Iberian Peninsula is the predominant feature impacting the GOL and Bay of Biscay. If strong enough, it would suggest that southeasterly flow could be in the GOL yet northwesterly flow is what is indicated in the wind data. I believe that the model is trying to suggest that the high pressure system located over northern Germany is driving light northwesterly winds over the GOL. However, that is not able to be deduced due to weak gradient depicted in the model projection. As we see from 4.9, the combination of this weak high over Northern Germany and the strong Azores high ridging into the area

48

is the synoptic setup that occurs. In Fig. 4.17 a return to the synoptic picture in Fig 4.13 is apparent but with stronger ridging from the Azores high over the Bay of Biscay and into western France. Northwesterly winds are apparent in the GOL. The weak high over Germany shown in Fig. 4.16 is now a weak ridge with no closed isobar but the net impact on the GOL is northwesterly indicating a Mistral. In our final projection, Fig. 4.18 the Azores high pressure system has ridging much farther west than in previous runs and not as it was depicted in Fig. 4.9. The gradient between the ridge and the low pressure system over Scandinavia is causing northwesterly flow into the GOL and appears to be enhanced by leeside troughing over Italy. No weak high over Northern Germany is projected as it occurred in Fig. 4.9. Although each of these plots suggests northwesterly flow over the GOL and would definitely suggest to a forecaster that a Mistral event was likely, the vacillation between model runs is too severe for the forecaster to identify the synoptic setup on this or any other particular day during the six day event.

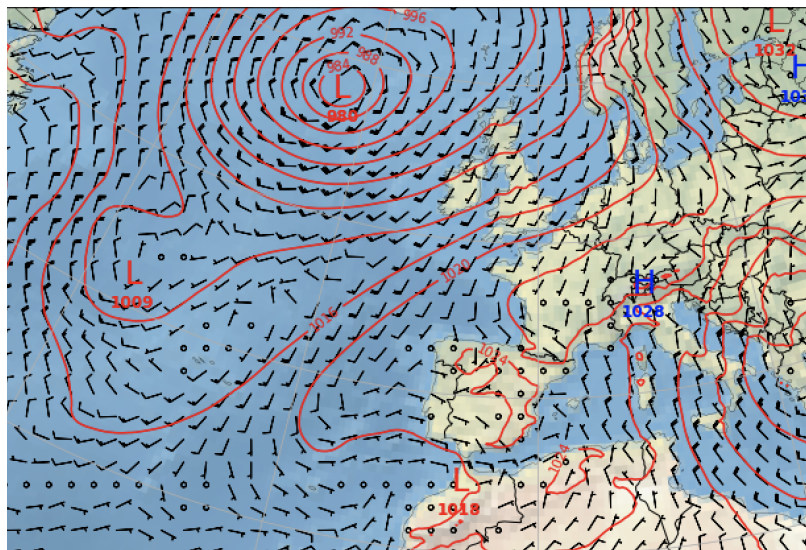### 4.3.2 Mistral Event: October 22-24, 2017

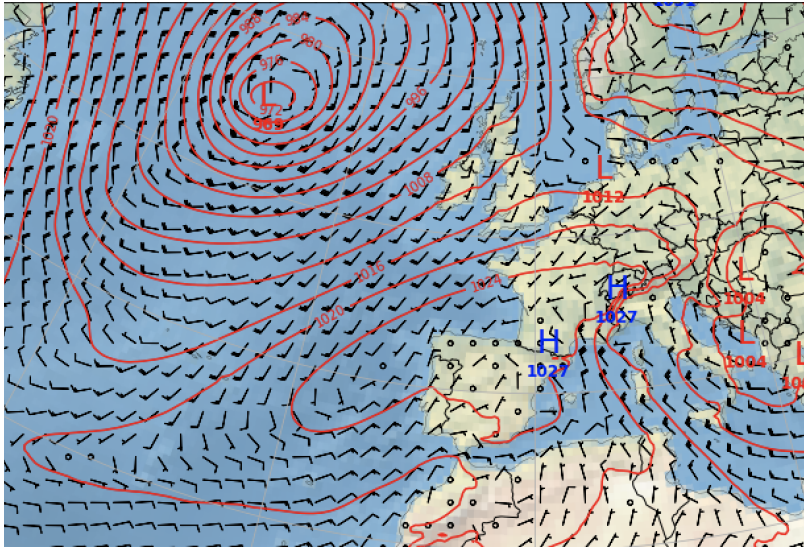Figure 4.19. ERA5 reanalysis plot for 10-22-2017.

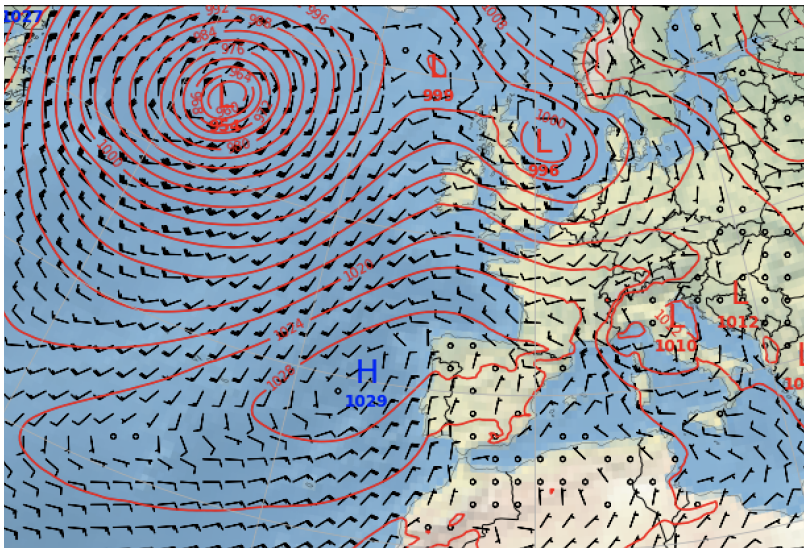Figure 4.20. ERA5 reanalysis plot for 10-23-2017.

Figure 4.21. ERA5 reanalysis plot for 10-24-2017.

In this event, shown in Figs. 4.19-4.21, a type B Mistral event resulting from a type A (Fig. 2.3) occurred with a closed low pressure system over Northern Italy (Genoa Low) in Fig. 4.21. Based on our analysis of the Surface Pressure mb spread at Perpignan, Marseille, and Nice (Fig. 4.9) there is a strong indication that ESPC will display skill at predicting this

event in the forecast window of 7-21 days. As the previous example Sec. 4.3.1 illustrated, the ability of the low pressure systems to be accurately depicted will be the challenge in identifying the synoptic setup. This event shows a mature low pressure system in the North Atlantic that was similar to the complex area of low pressure systems in Sec. 4.3.1. Identifying the ridging pattern into Eastern Europe will be the challenge for ESPC in this event. Just as in the previous example in Sec. 4.3.1, all plots were analyzed but one day is shown for brevity. In this case, we will analyze the model projections for 10-23-2017 during the highest intensity of the three day Mistral event.
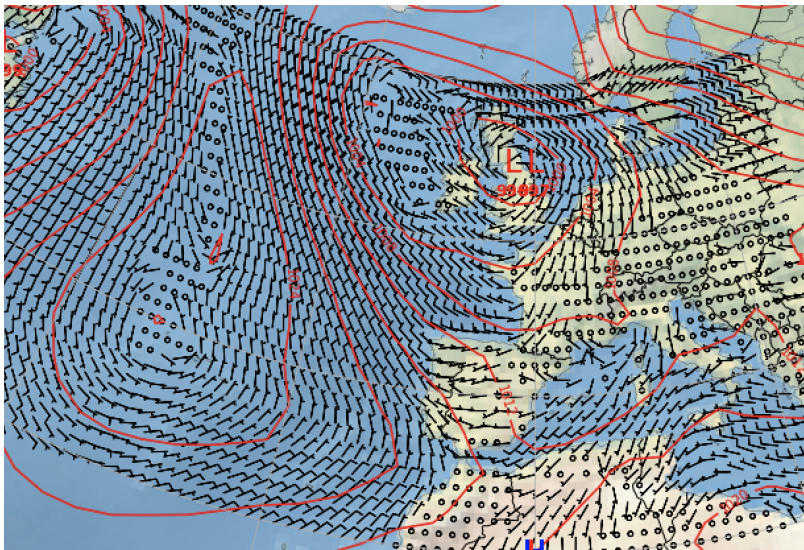

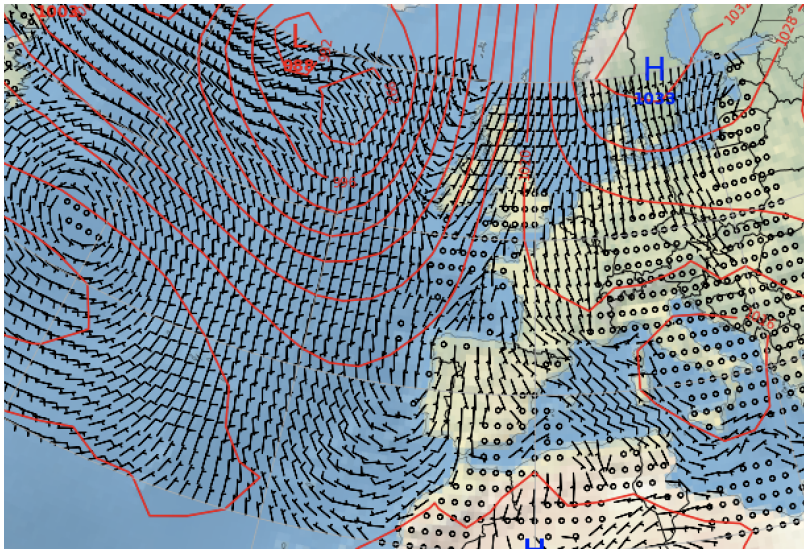Figure 4.22. ESPC forecast plot for 10-23-2017 produced on 10-01-2017

Figure 4.23. ESPC forecast plot for 10-23-2017 produced on 10-02-2017
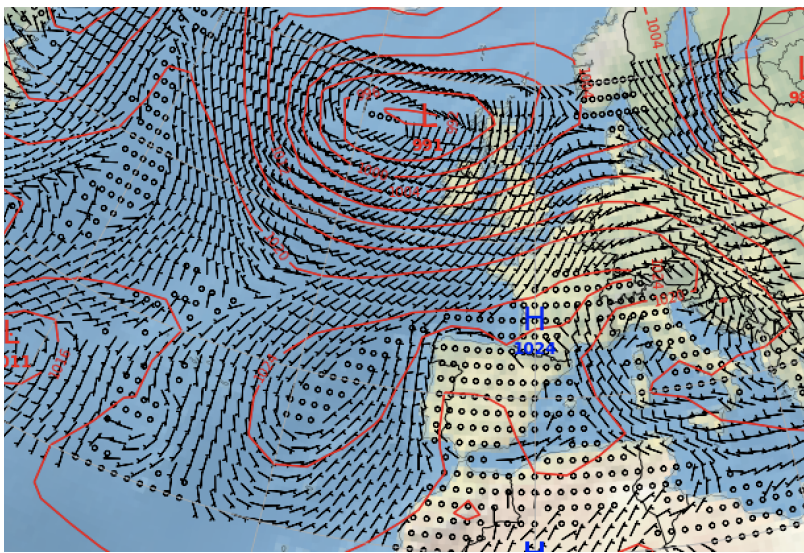

Figure 4.24. ESPC forecast plot for 10-23-2017 produced on 10-03-2017

Figure 4.25. ESPC forecast plot for 10-23-2017 produced on 10-07-2017

Figure 4.26. ESPC forecast plot for 10-23-2017 produced on 10-08-2017
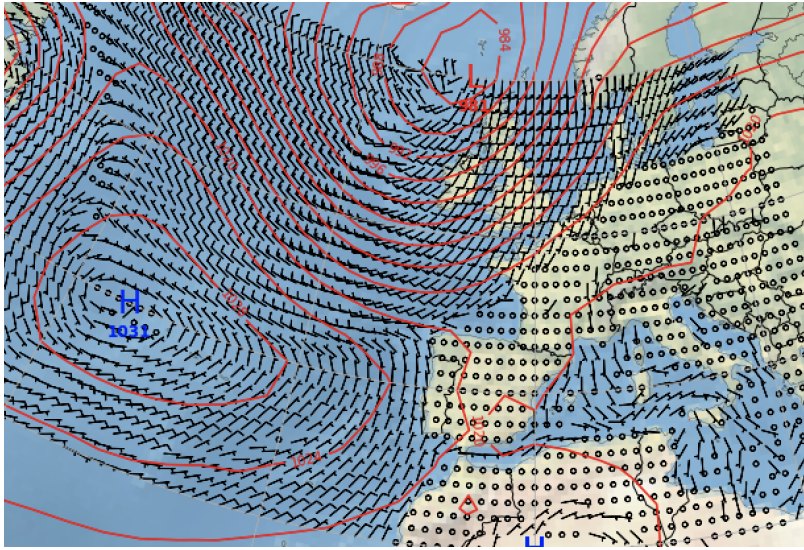
Figure 4.27. ESPC forecast plot for 10-23-2017 produced on 10-09-2017

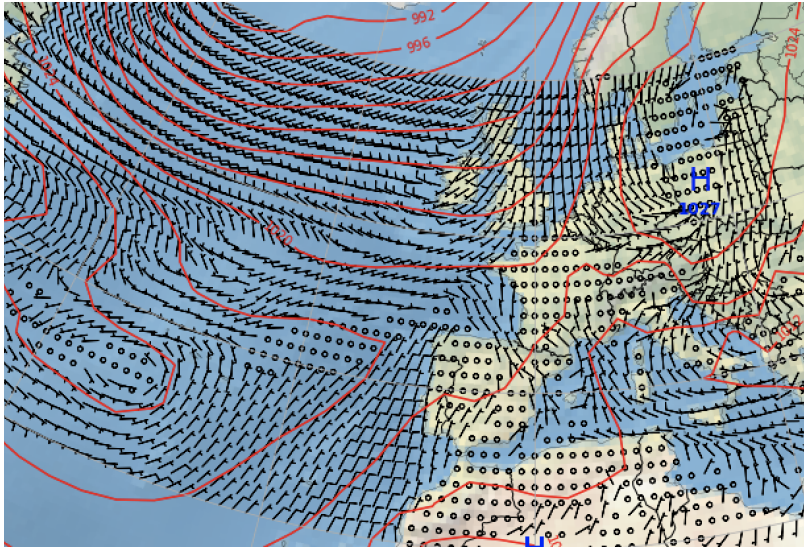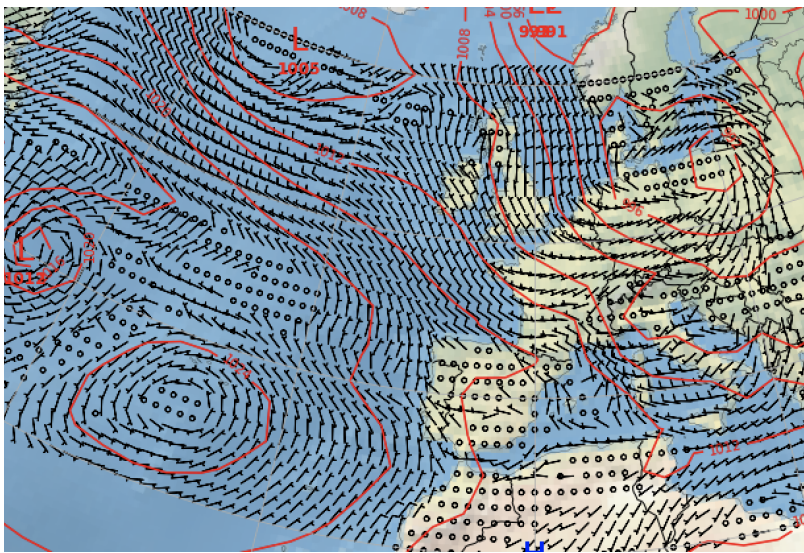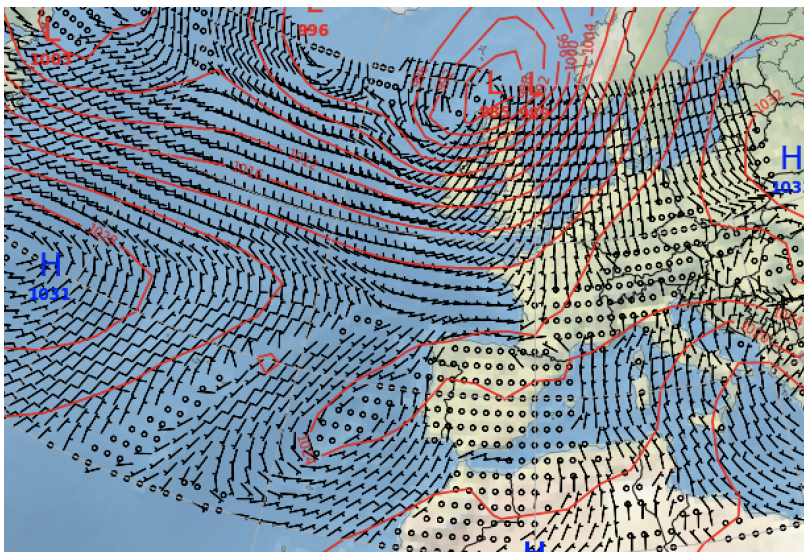Figure 4.28. ESPC forecast plot for 10-23-2017 produced on 10-10-2017
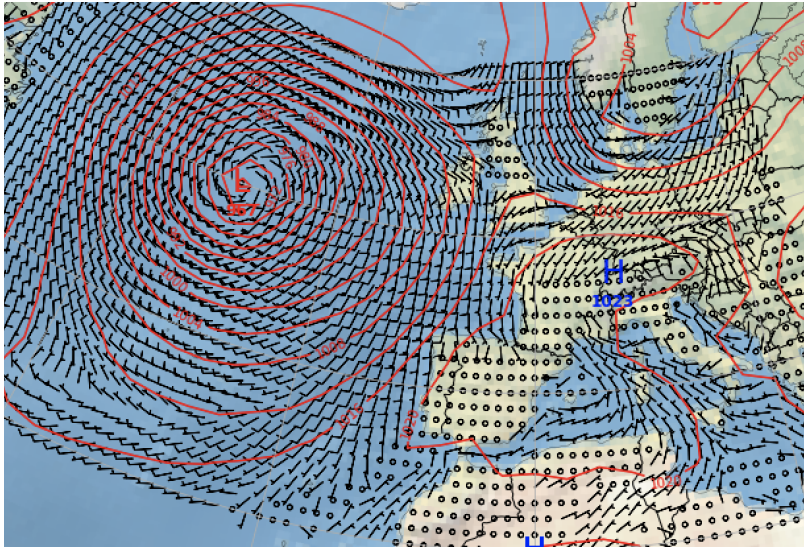
Figure 4.29. ESPC forecast plot for 10-23-2017 produced on 10-14-2017
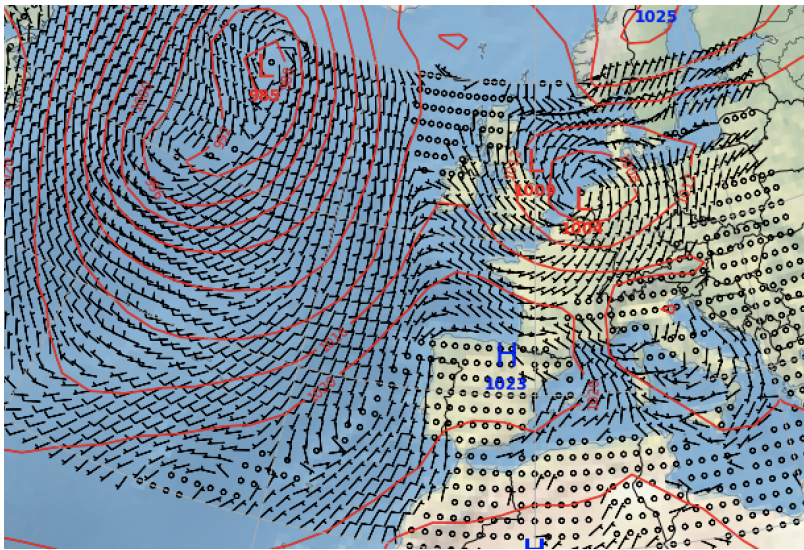
Figure 4.30. ESPC forecast plot for 10-23-2017 produced on 10-15-2017

In this series of plots all valid on 10-23-2017, we begin by looking at Fig. 4.22 where a complex area of low pressure seems to be dominating the North Sea area and over Great Britain. The Azores high is ridging north into the North Atlantic and an area of cyclonic circulation appears to be in the GOL with no apparent Mistral event indicated. The next Fig.

4.23 displays the same area of complex low pressure further west with southeasterly flow over the GOL. There is a high pressure center over the Baltic Sea and tight gradient between it and the low to the west but neither should have an impact as far south as the GOL. In the next plot, Fig. 4.24 a high pressure center has appeared over the Bay of Biscay with another area of anti-cyclonic flow over the Azores and is generating northwesterly winds in the GOL. The strong area of low pressure in the North Atlantic is showing to be west of Ireland and tightening a horizontal gradient between the Azores high and itself. This is very close to the surface picture depicted in Fig. 4.20. In the next plot, Fig. 4.25 light northerly winds are apparent in the GOL and the aforementioned low in the North Atlantic is not depicted. A tightened gradient between, what we assume to be the low in the Arctic region and the Azores high, is shown over the North Atlantic but the Mistral conditions are not as well depicted as they were in Figs. 4.23 and 4.24. In the next plot, Fig. 4.26 northwesterly flow is depicted more towards the islands of Corsica and Sardinia than in earlier model runs with areas of lighter or confused winds off of the Spanish coastline. Strong ridging from the Azores high is not apparent and complex areas of low pressure have remained in the North Atlantic and North Sea. In the next plot, Fig. 4.27 the mid-Atlantic high is shown interacting with a now uniform mature low pressure system in the North Sea and Arctic Region. However, this gradient is not producing Mistral conditions in the GOL as light southerly flow is projected to be in the area. In the final plot, Fig. 4.29, the mid-Atlantic high is now shows very far to the west while the low pressure area of interest in the North Sea is now projecting a tightened gradient to produce zonal winds into the Bay of Biscay before becoming too weak to produce a Mistral event. In this event, ESPC had correctly identified an instance where a Mistral event was likely to occur in early model runs but the later model runs lost agreement and could not identify the proper synoptic setup that took place and caused a Mistral event to occur on this day.
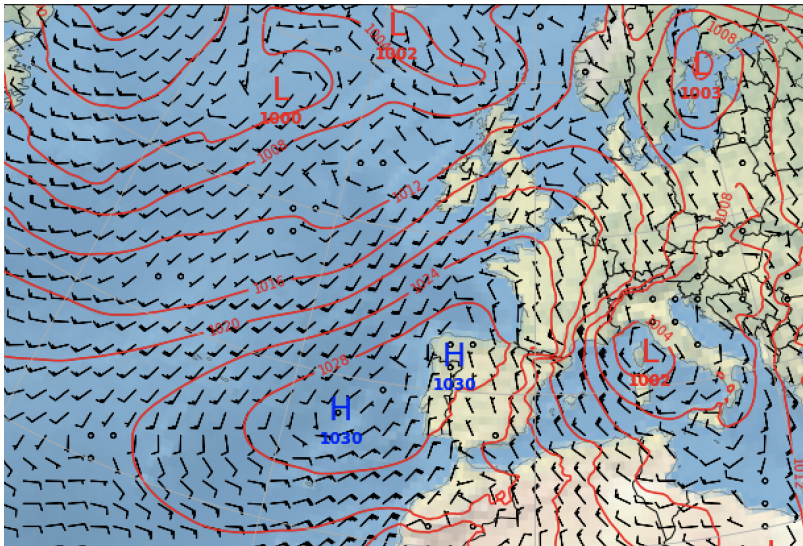
4.3.3 Mistral Event: February 3, 2019

Figure 4.31. ERA5 reanalysis plot for 02-03-2019.

In this figure (Fig. 4.31), a type B Mistral (Fig. 2.3) is depicted with a ridging high pressure system over the Iberian Peninsula and into the GOL. A closed Genoa low pressure system enhances the northwesterly flow and a horizontal gradient along southern France is visible and within our contingency table shown in Table 4.8. The enhancement of the northwesterly winds in the GOL is being initiated by the tightened gradient between these two areas of high and low pressure with the cyclonic flow for the low enhancing wind speeds enough to impact the daily averaged wind speed in the GOL. The daily averaged wind speed, according to ERA5 reanalysis data, was over 41 kts. Additionally, the days surrounding this event also saw intense wind speeds although not from the direction indicating a Mistral. Given the nature of this event, it represents how Mistral events can accompany other dynamically important conditions in the GOL.

Figure 4.32. ESPC forecast plot for 02-03-2019 produced on 01-15-2019

Figure 4.33. ESPC forecast plot for 02-03-2019 produced on 01-19-2019

Figure 4.34. ESPC forecast plot for 02-03-2019 produced on 01-20-2019
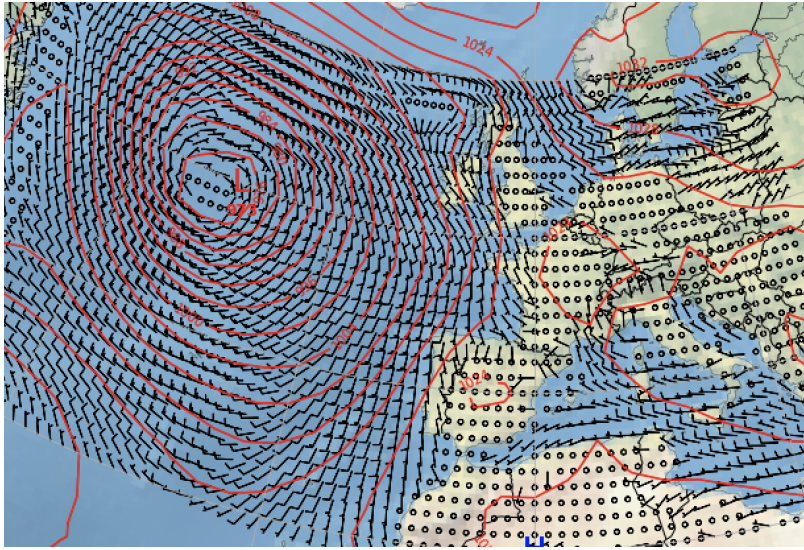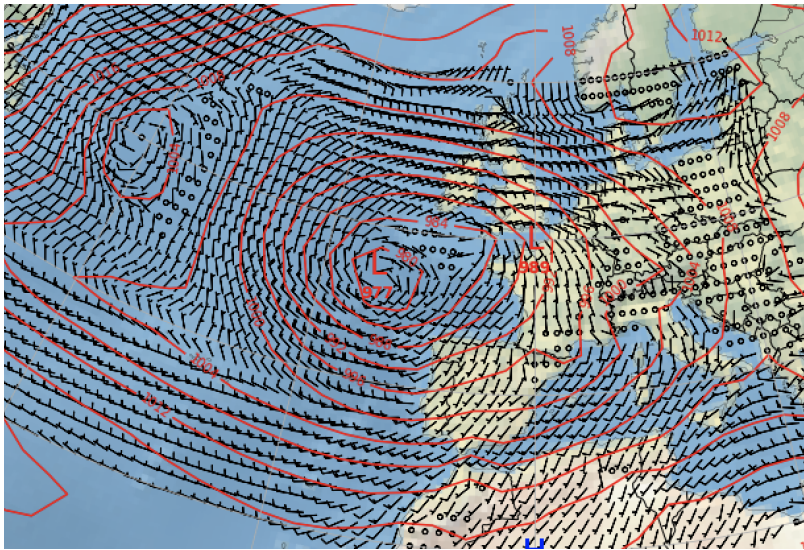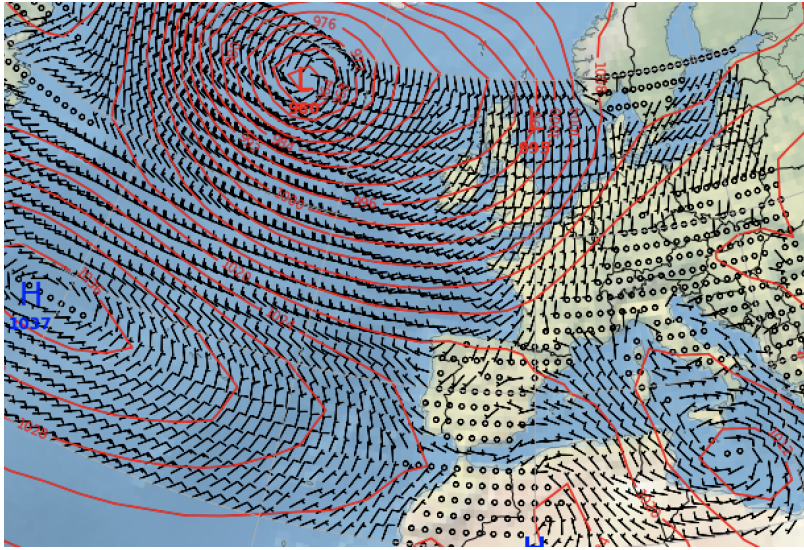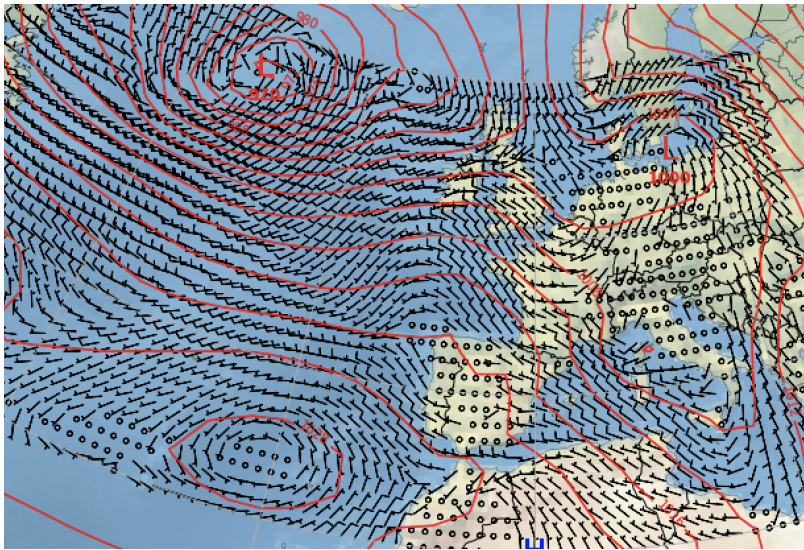

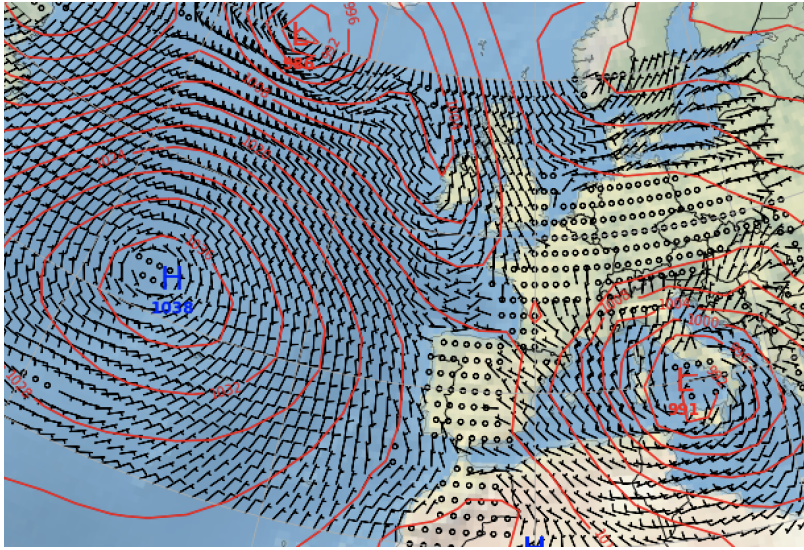Figure 4.35. ESPC forecast plot for 02-03-2019 produced on 01-21-2019

Figure 4.36. ESPC forecast plot for 02-03-2019 produced on 01-22-2019
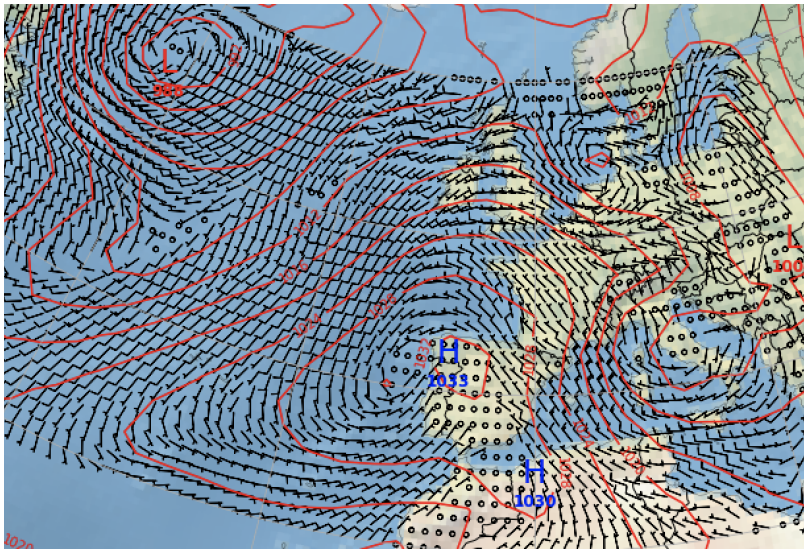

Figure 4.37. ESPC forecast plot for 02-03-2019 produced on 01-26-2019
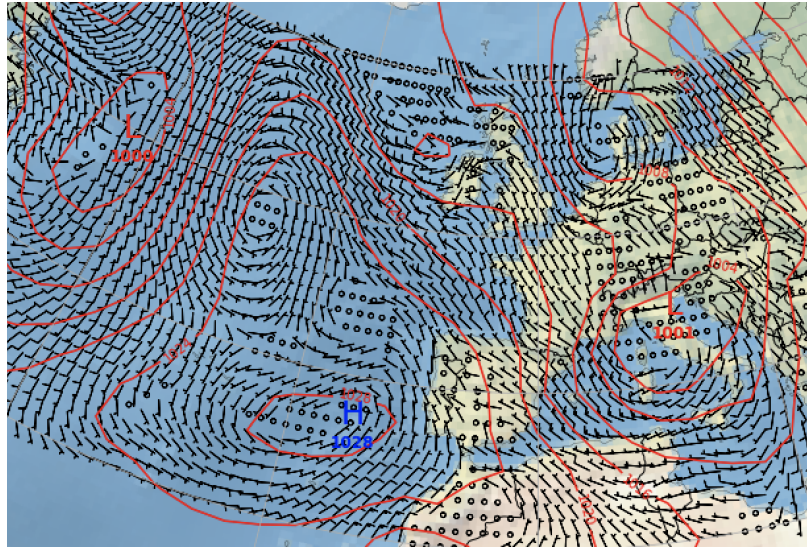
Figure 4.38. ESPC forecast plot for 02-03-2019 produced on 01-27-2019

In this series of plots all valid on 02-03-2019, we begin by looking at Fig. 4.32 where a very strong low pressure system is depicted as influencing all of the synoptic picture of the North Atlantic. An area of light and confused winds appears over most of France with light northwesterly winds in the GOL. In the next plot, Fig. 4.33, the low is depicted as a complex area of low pressure further to the east and over the western portion of France which is bringing southwesterly flow to the GOL. In the next plot, Fig. 4.34, the area of low pressure has moved north and is interacting with a strong high in the mid-Atlantic. This is causing a tightened gradient to bring zonal flow to the eastern Bay of Biscay with southerly winds ahead of an assumed cold front extending from the low pressure system over eastern Britain. There is a strong North African cyclone entering the central Mediterranean and is being depicted as the feature causing northwesterly winds to be forecast in the GOL. In the next plot, Fig. 4.35, the high pressure system has moved east and is being depicted with ridging into the Bay of Biscay and, along with an area of cyclonic flow over Italy, causing northwesterly flow over the GOL. In the next plot, Fig. 4.36, the high pressure system is now further to the northwest and has a strong ridge extending north. A closed low pressure system over southern Italy is strong and causing northwesterly flow over the GOL. Winds over most of France and the Iberian Peninsula are light and confused and do not suggest that a tightened gradient is causing a Mistral event but only the winds associated with the low

61

pressure system. In the next plot, Fig. 4.37, strong ridging from a high pressure center over the northwest corner of the Iberian Peninsula is shown enhanced by a low over southern Italy very close to the reanalysis projection shown in Fig. 4.31 with some minor differences in intensity and placement of the low and high pressure centers. The final plot, Fig. 4.38, shows a strong ridge returning from Fig. 4.36 but with the same gradient from Fig. 4.37 and a similarity in northwesterly wind intensity in the GOL. These plots indicate another example of how ESPC can display the net impact of Mistral winds in the GOL despite mis-identifying the correct synoptic setup responsible for the Mistral event.

CHAPTER 5:
Discussion and Future Work

5.1 Discussion

Based on the results discussed in Chapter 4, there is not an appreciable amount of skill in the raw wind data at the GOL buoy location inherent in the ESPC model, as shown in Section 4.1, that is above the inherent rate of 17% that climatology suggests in Section 3.1. By splitting the data into windows of 7-14 and 14-21 days, the data does not seem to suggest any large increase in skill either (see Tables 4.3 and 4.2) with PODs of .120 and .091, respectively.

When the addition of the thumb rules from Brody and Nestor (1980) were added, we saw gains in POD above climatology for the surface pressure spread at Perpignan, Marseille and Nice as well as the 850 mb wind speed and intensity rules that were verified by ERA5 reanalysis data using the same criteria. However, the 500 mb winds at Brest and Bordeaux rule did not yield any results and also did not verify as a valid measure of prediction based on an analysis of ERA5 data. The forecaster thumb rules that displayed utility verified by ERA5 reanalysis and the raw ESPC wind data suggest that there is inherently a high FAR associated with this POD. This suggests that ESPC has a high bias when using thumb rules but not when using raw model data. The data from Sections 4.1 and 4.2 illustrate ESPC's tendency to forecast for Mistral Events during the period of our study relative to the climatological rate of 17% would not provide a reliable method of forecasting Mistral events in the 7-21 day time frame. The thumb rules, however, show skill above climatology, despite high bias, when added to the forecast process.

The plots outlined in Section 3.2.3 illustrate the atmospheric chaos being portrayed by ESPC in this single deterministic run. Although, there are periods of northwesterly winds portrayed in these model runs, the synoptic reasoning was not properly identified to the setups described in Fig. 2.3. Therefore, we cannot conclude that ESPC displayed capabilities of properly identifying the correct synoptic setup that induced Mistral events as we hypothesized.

63

Given the course of this research to study the ability of deterministic ESPC to detect a Mistral event in the GOL within the forecast window of 7-21 days for a known period of at least 1 day, the forecaster would be best suited to utilize the surface pressure spread for Perpignan, Marseille, and Nice or the Nîmes 850 mb winds forecaster thumb rules than raw ESPC model wind output. The high FAR also needs to be added as a caveat to both methods as well. The confidence level would be dependent on the forecaster's familiarization with the Mistral and the thumb rules contained wherein. However, I do not believe that a determination could be made until the latter portion of the forecast window and therefore do not place the skill for this event beyond current global NWP models. There is too much ambiguity in this dataset to suggest that deterministic ESPC adds any skill beyond current long-range global models without introducing the increased possibility of a false alarm or missed event.

Due to limitations of the IRI data base, a single deterministic forecast was used when a probabilistic approach from the 16-member ensemble would likely have been more skillful. Atmospheric chaos, especially at long lead times, meant that the forecast, even in the vicinity of the high pressure systems, was unable to capture the relative strength of low pressure systems with enough accuracy to deduce the synoptic picture. Probabilistic information from an ensemble would be more appropriate to use. Such a model is currently available but only has been operational since August of 2020 and not enough data would have existed at the time of study to utilize this approach. I anticipate that ensemble forecasts would display a skill beyond those of a deterministic approach and each of these methods could be used to calculate predictive measures should the forecaster choose a probabilistic approach as well.

5.2   Future Work

Efforts to add the NAO index to the ESPC model output are currently being developed by NRL. A similar test using this method could be beneficial to compare the results and an assumed increase in skill with the added index. This will allow us to visualize the change to the same metrics in order to see refinement in the results. I believe that due to the reliance of each synoptic setup to the relative strength of the Azores high pressure system is a key to understanding the likelihood of a Mistral event that was never fully connected to the NAO in this study. My researching the index's impact to Mistral events in the context of the relative

strength of the 500mb heights of the Azores high pressure center might be the single metric needed to connect the synoptic pattern to Mistral likelihood. The chance that it improves the forecast results, I believe, is high and is worthy of further study.

In selection of the forecaster thumb rules of Brody and Nestor (1980), I chose to select instances that could be easily coded using observations and reanalysis data. Most of the rules involved analysis of pressure surfaces at various levels of the atmosphere in order to identify ridging and troughing over geographical locations. Due to the complexity in coding that into a contingency test, this type of test was not attempted and further study of that method of analysis using ESPC forecasts and ERA5 reanalysis data could be considered by another study. In particular, I believe this type of analysis would frame the results of 500mb winds at Brest and Bordeaux into further dynamical context that the simple contingency table was unable to do. Additionally, I believe some of the simple tests for 500mb wind direction and speed were not as accurate as they could have been in conjunction with a test for ridging over the area as the original rules suggest. Further tests of a similar manner are needed to properly evaluate the accuracy of the rules before disregarding their initial accuracy.

Synoptic level wind events such as monsoonal flow over southeast Asia and gap wind events in other areas of the world could also be studied in a similar manner as used in this research. Repeating the method of raw model output comparison, contingency table using forecast metrics, and practical surface analysis can be useful tools in order to identify the onset of other events in order to expand the utility of ESPC and S2S forecasts to operational forecasters. The current usage of MJO phase in ESPC model output may contribute to a connection between the current phase of the oscillation and an increase in forecast accuracy of wind events in the area and provide clues to improving the results of this study as well.

THIS PAGE INTENTIONALLY LEFT BLANK

List of References

Allard, R., and Coauthors, 2020: Analyzing the impact of cryosat-2 ice thickness initialization on seasonal Arctic Sea ice prediction. *Annals of Glaciology*, **61 (82)**, 78–85.

Barton, N., M. Janiga, J. McLay, C. Reynolds, C. Rowley, P. Hogan, and P. Thoppil, 2019: Earth system prediction capability (espc) initial operational capability (ioc) ensemble system. Tech. rep., NAVAL RESEARCH LAB MONTEREY CA MONTEREY United States.

Bretschneider, C., 1970: Forecasting relations for wave generation. *Look Lab/Hawaii*, **1 (3)**, 31–34.

Brody, L. R., and M. J. R. Nestor, 1980: *Handbook for Forecasters in the Mediterranean. Part 2. Regional Forecasting Aids for the Mediterranean Basin*. NAVAL ENVIRONMENTAL PREDICTION RESEARCH FACILITY MONTEREY CA.

Brunet, G., and Coauthors, 2010: Collaboration of the weather and climate communities to advance subseasonal-to-seasonal prediction. *Bulletin of the American Meteorological Society*, **91 (10)**, 1397–1406.

Chassignet, E. P., H. E. Hurlburt, O. M. Smedstad, G. R. Halliwell, P. J. Hogan, A. J. Wallcraft, R. Baraille, and R. Bleck, 2007: The hycom (hybrid coordinate ocean model) data assimilative system. *Journal of Marine Systems*, **65 (1-4)**, 60–83.

Dedecca, J. G., R. A. Hakvoort, and J. R. Ortt, 2016: Market strategies for offshore wind in europe: A development and diffusion perspective. *Renewable and Sustainable Energy Reviews*, **66**, 286–296.

Eleuterio, D. P., and S. Sandgathe, 2012: The earth system prediction capability program. *2012 Oceans*, 1–3, doi: 10.1109/OCEANS.2012.6404895.

Givon, Y., D. Keller Jr, V. Silverman, R. Pennel, P. Drobinski, and S. Raveh-Rubin, 2021: Large-scale drivers of the mistral wind: link to rossby wave life cycles and seasonal variability. *Weather and Climate Dynamics*, **2 (3)**, 609–630.

Google, 2022: Gulf of lion to tyrrehnian sea. Google, URL https://earth.google.com/web/@40.65776798,7.58902423,31.35858457a,1712570.33775955d,35y,-0h,0t,0r.

Hersbach, H., and Coauthors, 2020: The era5 global reanalysis. *Quarterly Journal of the Royal Meteorological Society*, **146 (730)**, 1999–2049.

Hunke, E. C., W. H. Lipscomb, A. Turner, N. Jeffery, and S. Elliott, 2008: Cice: The Los Alamos sea ice model, documentation and software user's manual. *T-3 Fluid Dynamics Group, Los Alamos National Laboratory, Los Alamos, NM*, **87545**, 505.

Hurrell, J., G. A. Meehl, D. Bader, T. L. Delworth, B. Kirtman, and B. Wielicki, 2009: A unified modeling approach to climate system prediction. *Bulletin of the American Meteorological Society*, **90 (12)**, 1819–1832.

Iseh, A., and T. Woma, 2013: Weather forecasting models, methods and applications. *International Journal of Engineering Research & Technology*, **2 (12)**, 1945–1956.

Janiga, M. A., C. J. Schreck III, J. A. Ridout, M. Flatau, N. P. Barton, E. J. Metzger, and C. A. Reynolds, 2018: Subseasonal forecasts of convectively coupled equatorial waves and the mjo: Activity and predictive skill. *Monthly Weather Review*, **146 (8)**, 2337–2360.

Lamb, P. J., and R. A. Peppler, 1987: North Atlantic oscillation: concept and an application. *Bulletin of the American Meteorological Society*, **68 (10)**, 1218–1225.

Liang, P., and H. Lin, 2018: Sub-seasonal prediction over east Asia during boreal summer using the eccc monthly forecasting system. *Climate Dynamics*, **50 (3)**, 1007–1022.

Madden, R. A., and P. R. Julian, 1972: Description of global-scale circulation cells in the tropics with a 40–50 day period. *Journal of Atmospheric Sciences*, **29 (6)**, 1109–1123.

May, R. M., and Coauthors, 2022: Metpy: A Python package for meteorological data. Unidata, urlhttps://github.com/Unidata/MetPy, doi: 10.5065/D6WW7G29.

Met Office, 2010 - 2015: *Cartopy: a cartographic python library with a Matplotlib interface*. Exeter, Devon, URL https://scitools.org.uk/cartopy.

Reiter, E. R., 1975: *Handbook for forecasters in the Mediterranean*. Environment Prediction Research Facility, Naval Postgraduate School.

Roebber, P. J., 2009: Visualizing multiple measures of forecast quality. *Weather and Forecasting*, **24 (2)**, 601–608.

Ruti, P. M., and Coauthors, 2020: Advancing research for seamless earth system prediction. *Bulletin of the American Meteorological Society*, **101 (1)**, E23–E35.

Shapiro, M., and Coauthors, 2010: An earth-system prediction initiative for the twenty-first century. *Bulletin of the American Meteorological Society*, **91 (10)**, 1377–1388.

Theurich, G., and Coauthors, 2016: The earth system prediction suite: Toward a coordinated us modeling capability. *Bulletin of the American Meteorological Society*, **97 (7)**, 1229–1247.

Walker, G. T., and E. Bliss, 1933: Discussion of memoirs. *Quarterly Journal of the Royal Meteorological Society*, **59 (249)**, 163–165.

THIS PAGE INTENTIONALLY LEFT BLANK

Initial Distribution List

1. Defense Technical Information Center
   Ft. Belvoir, Virginia

2. Dudley Knox Library
   Naval Postgraduate School
   Monterey, California